Ultraviolet Low-Resolution Spectropolarimeter for the Space Mission Spectrum-UV (UVSPEPOL Project)

V. A. Kucherov[1], Yu. S. Ivanov[1], Yu. S. Efimov[2], A. V. Berdyugin[2], N. M. Shakhovskoy[2]

[1] Main Astronomical Observatory of the National Academy of Sciences of Ukraine
[2] Crimean Astrophysical Observatory, Ukraine

INTRODUCTION

It is well known that polarimetric measurements give essential information which is important in solving many problems in the physics of the Universe. Such information cannot be obtained from any other kind of observations. Indeed, within the optical region, one may remind that just the discovery and investigation of interstellar polarization of stellar light made a substantial contribution to the ideas on geometry and composition of interstellar dust grains and gave the first knowledge about the structure of the global magnetic field of the Galaxy; owing to the discovery of polarization of the continuum radiation from the Crab nebula, the nature of this emission was finally established and the first nonthermal mechanism of radiation — synchrotron radiation of relativistic electrons in magnetic fields — was introduced into astrophysics; the detection of strong polarization of the radiation from close binary systems of the AM Her type led to the discovery of large-scale magnetic fields with huge field intensities equal to a few tens of megagauss, which is a crucial factor for geometry shaping of the system, and cyclotron frequencies turned out to be in the optical spectral region. Polarimetric results obtained and analyzed till the present day showed that such measurements were very efficient in solving such tasks as the diagnostics of nonthermal radiation mechanisms, determination of the spatial structure of matter and radiation field distribution in the objects of small angular sizes, and determination of the optical, physical, and chemical properties of circumstellar, interstellar, and intergalactic grains.

Necessity for solving these tasks — taken separately and in various combinations — appears while studying very different astrophysical objects — from comets and asteroids to quasars, blazars, and intergalactic diffuse matter.

The present-day polarimetry has a substantial gap just in the ultraviolet spectral region. Polarimetric observations in the ultraviolet are much more complicated than analogous ground-based observations in the visible wavelength region. This is clearly seen from the fact that many astrophysical objects seem to be different at different frequencies. Thus, for instance, contribution of stellar components to the total radiation of active extragalactic systems changes significantly with wavelength. The wavelength dependence of polarimetric properties of cosmic grains strongly varies, and the change of wavelength interval by factor 2 or 3 may result in the replacement of one

plasma radiation mechanism by another. Therefore, for a better understanding of the nature of such objects it is necessary to use polarimetric data both in the optical and ultraviolet wavelength regions.

These general reasons may be supported by two specific facts from the current space research.

1. Two quite unexpected results were obtained in the course of the Wisconsin Ultraviolet PhotoPolarimeter Experiment (WUPPE) observations lasting only 8 hours (see below for a detailed description). First, it was revealed that the wavelength dependence of polarization of hot stars in the ultraviolet is incompatible with the generally accepted model of the origin of polarized radiation, and second, some peculiarities which are due to strong absorption of polarized radiation by a circumstellar envelope were detected in the emission spectra of these stars.

2. Practically all devices aboard the Hubble Space Telescope (HST) initially have had the polarimetric modes which allow direct images and spectra to be obtained in polarized light.

All these reasons make the polarimetric investigations aboard the Space Telescope T-170 within the framework of the SPECTRUM-UV experiment (Boyarchuk and Tanzi, 1993; Gershberg et al., 1995) very promising. Using a telescope with a primary mirror 1.7 m in diameter on the station in a high-apogee orbit, it is possible to observe much fainter sources than it was possible in the WUPPE short-time missions when a telescope with a 0.5-m primary mirror was used, to carry out observations far beyond the radiation belts and magnetosphere of the Earth, thus avoiding their negative influence on measurements, to make monitoring of weak objects which are difficult to observe with the HST. SPECTRUM-UV will have a great advantage of its orbit, contrary to the HST. This gives us unique opportunity to have a monitoring time of several days for selected object instead of that of about 20 minutes with HST. Thus one can see that the Ultraviolet low-resolution spectropolarimeter (UVSPEPOL) experiment may produce results which will significantly exceed other polarimetric investigations performed or planned for the nearest decades.

The present document consists of three parts. In the first part, scientific grounds for the UVSPEPOL experiment are given: we review the present state of polarimetry in the ultraviolet and propose some scientific tasks which are expected to be solved during this experiment.

In the second part some design models of existing ultraviolet polarimeters are described and compared.

In the third part original systems of low-resolution ultraviolet polarimeter within the framework of the SPECTRUM-UV experiment concept are considered.

This document is based on the analyses of various aspects of this problem which were made earlier at the Crimean Astrophysical Observatory, Main Astronomical Observatory, National Academy of Sciences of Ukraine, and Central Astronomical Observatory, Russian Academy of Sciences (Kucherov et al., 1995; Kucherov and Efimov, 1996; Steshenko, 1996; Gnedin, 1996).

PART 1.
THE PRESENT STATE OF POLARIMETRIC RESEARCH IN THE ULTRAVIOLET AND SCIENTIFIC OBJECTIVES FOR THE UVSPEPOL EXPERIMENT

First polarimetric measurements outside the atmosphere were made in 1966—1972 by T. Gehrels (1974) with a balloon ultraviolet polarimeter and by P. Stecher (1972) with a rocket ultraviolet polarimeter. The purpose of those experiments was to check the behaviour of the parameters of interstellar linear polarization in the ultraviolet. Later a series of space experiments followed, with the polarization of the Sun and the solar corona studied in the wavelength region 120—350 nm (Stenflo et al., 1976; Gountail, 1978; Stenflo et al., 1980; Miller et al., 1981). As a continuation of these investigations, a wide-angle panoramic L_α coronograph-polarimeter (Lya CoPo) is intensively developed at present in the USA. It is intended for studying magnetic fields in active features of the solar corona (Fineschi et al., 1991; Hoover et al., 1991, 1992, 1993).

As to astrophysical objects beyond the solar system, excepting a pioneer paper by Gehrels, the first large program on the research of polarization in the ultraviolet region was initiated in 1990. These works started and still go on at the Laboratory of Space Astronomy in the Wisconsin University. In the course of a 9-day flight of the ASTRO-1 observatory equipped with an ultraviolet polarimeter (WUPPE) aboard the Space Shuttle Columbia polarimetric measurements (8 hours in total) of more than 20 galactic and extragalactic objects were carried out.

There are wide opportunities for polarimetric measurements in the ultraviolet aboard the successfully working HST. In contrast to WUPPE aimed to study the UV polarization of bright objects, the HST polarimetric facilities were designed to make observations with high spatial resolution and to give the opportunity to observe faint objects.

1.1. Results of polarimetric observations obtained in the WUPPE experiment and with the HST

The purpose of the ASTRO-1 mission was to study the polarization of the interstellar dust, intrinsic polarization of rapidly rotating Be-stars, polarization of active galactic nuclei and some other objects. Table 1 presents the list of principal WUPPE observations.

Ultraviolet observations carried out in the WUPPE experiment were accompanied by precise ground-based polarimetric measurements in the visible spectral region with a spectropolarimeter of analogous design at the Pine Bluff Observatory.

By now a large cycle of unique astrophysical investigations has been performed with polarimeters aboard the HST, they are listed in Table 2 (see Part 2). In particular, the polarization of the interstellar dust, of BL Lac-type objects (blazars), of selected quasars and active galactic nuclei (AGNs) was studied (Allen et al., 1993; Smith et al., 1993a, 1993b; Somerville et al., 1994).

A brief review of major results from polarimetric observations of galactic and extragalactic objects with the WUPPE and HST is given below.

Table 1. List of Polarimetric Observations Made in the WUPPE

Types of objects	Objects	Description of results
Polarimetric standards	γ Gem,	
	HD 25443	Clayton et al., 1992
Supergiants	κ Cas	Taylor et al., 1991
	α Cam	Clayton et al., 1992
	α Ori	Nordsieck et al., 1994
	HD 45677	Schulte-Ladbeck et al., 1992b
	P Cyg	Taylor et al., 1991
Be-stars	ζ Tau	Bjorkman et al., 1991
	ρ Car	Bjorkman et al., 1993
	φ Aqr	Bjorkman et al, 1991
Wolf-Rayet stars	EZ CMa	Schulte-Ladbeck et al., 1992a
	θ Mus	Schulte-Ladbeck et al., 1992a
Rapidly rotating stars	α Hui	
	φ Vel	
White dwarf	Gr+70 8247	
Stars with chromospheric activity	α Aur	
Cataclysmic stars	UX UMa	
Planetary nebula	NGC 1535	
Reflective nebula	NGC 7023	
Interstellar polarization	HD 37903	
	HD 62542	
	HD 99264	
	HD 197770	Clayton et al., 1992
Normal galaxies	M 31	
	M 33	
	M 74	
	M 82	
Active galaxies	Mkn 335	
	NGC 1068	Code et al., 1993
Quasars	3C 273	
	Q1821	

1.1.1. Extragalactic systems

Much attention was given in the last decade to the study of various types of active extragalactic objects — quasars, blazars, and AGNs. The majority of these objects are characterized by well-expressed variability of their brightness and polarization. It is believed that the activity of galactic nuclei is caused by the existence of black holes surrounded by accretion disks. The significant part of radiation from active nuclei arises in very small volumes, and its maximum is usually located in the UV region of the spectrum.

The HST polarimeters allow observations of the inner parts of AGNs, where major physical processes occur. Such observations would help essentially to understand the most difficult problems, such as the nature of central source, structure and physical properties of AGNs, the nature of the physical mechanisms which are responsible for the observed spectral features, etc. For example, the large (about 30 %) and variable polarization observed in blazars is connected with the dominant directional synchrotron radiation. Many AGNs have polarization which is usually considerably smaller (no more than 1—2 %), and its interpretation is not unequivocal. Various mechanisms are discussed: scattering of the light of nucleus on oriented dust particles and electron scattering. In many cases the problem is complicated by the contribution of nonpolarized radiation from the stellar component of the galaxy.

Appropriate models can be selected using polarimetric data in a wide spectral range.

Active galaxies

Some brightest AGNs which are well-studied in the optical region were selected for polarimetric observations in the ultraviolet with the HST. At present only the observations of two AGNs are published: NGC 1068 (type Seyfert 2) and MRK 231 (type Seyfert 1).

The difference between the types Seyfert 1 and Seyfert 2 was believed to be caused by the geometry of the circumnuclear region which is hidden by an optically thick dust torus. However, K. K. Chuvaev (Crimean Observatory) found that a galaxy of type Seyfert 1 changed to type Seyfert 2 during 2—3 months and then returned to the initial condition. This behaviour is inconsistent with the generally accepted model.

The most extensive observational run was obtained for NGC 1068 (Code et al., 1993; Antonucci et al., 1994; Capetti et al., 1994; Capetti et al., 1995). This galaxy is the brightest one among AGNs, so it was observed in the WUPPE and with the HST.

According to the model which was accepted for NGC 1068, the nucleus of type Seyfert 1 is located in the central region of the galaxy which is obscured by an opaque torus. The axis of symmetry of the torus is oriented parallel to radio jet direction. Emission from the broad line region and continuum source may emerge from the torus poles where it is scattered in the direction to the observer. This light is partially polarized during scattering, with the polarization plane perpendicular to the axis of symmetry of the torus.

In the diaphragms from 0.3" to 4.3" the ultraviolet polarization in the wavelength region from 160 nm to 280 nm is about 16 % at a position angle of 97°. From 280 nm to 330 nm the degree of polarization decreases to a level of about 11.5 %. This can be explained by the contribution from nonpolarized stellar light of the galaxy field. The polarization in narrow lines is considerably smaller than in the continuum — less than 2 %. The polarization in different lines was found to vary. So, the lines [C III] and Mg II have polarized components, while the forbidden line [Ne IV] 242.3 nm is not polarized. These polarimetric observations support the above-mentioned standard AGN model. The degree of polarization slightly varies with wavelength in the continuum, which suggests that the scattering by electrons is the main polarization mechanism. Comparison of the data obtained with different apertures indicates that the light scattering region has a size of about 1", which corresponds to about 10 parsecs.

The high spatial resolution of the HST observations offers the unique opportunity to investigate the structure of internal regions in details. The galaxy NGC 1068, one of the brightest among active galaxies, is the most suitable object for such studies. Since its nucleus is hidden by absorbing matter, an important problem is to determine the location of the galactic nucleus. Another important problem is to clarify the nature of grains which are responsible for the scattering of the light emitted from the nucleus. Since the scattered emission is polarized, polarimetric observations in the ultraviolet together with observations in the optical region can answer these questions. The observations were carried out on the HST with FOC. The polarization maps obtained show a central symmetrical picture which allows precise determination of the location of the galactic nucleus invisible in the optical region. The degree of polarization in the continuum is about 10 %, but in some regions it is as large as 60 %. After correction for dilution of polarization by nonpolarized stellar light it increases to 100 %. Two clouds with very high polarization were found at a distance of about 0.1" from the nucleus: polarization in the ultraviolet is about 43 %, while in the visible region it is only 9 %. It is possible that these clouds are connected with the active nuclear region (Capetti et al., 1994, 1995).

Spectropolarimetry of the galaxy MRK 231 was made with the FOS too. The polarization parameters in the ultraviolet are comparable with those which were obtained in ground-based observations in the visible spectral region: they are about 15 %. However, there are significant differences. The degree of polarization decreased by a factor of 2 from the centre of the line Mg II to its wings; it is not constant over the spectrum: the degree of polarization was about 17 % in the 270 nm region and decreased rapidly toward shorter wavelengths, and the polarization was absent at all at wavelengths shorter than 180 nm (Smith et al., 1994). A complicated shape of the polarization spectrum suggests that in the vicinity of the galactic nucleus the nonpolarized light from stellar components "dilutes" the polarization arising from strongly reddened nucleus. After correction for this effect the degree of polarization of the UV emission from the nuclear region exceeds 20 %. Besides, the rotation of the plane of polarization by 40° between 180 nm and 330 nm points to the presence of polarized clouds.

Blazars

Important information on blazars was obtained from the HST spectropolarimetry. Different assumptions were made as to the nature of their emission. One of them is the existence of an accretion disk around a black hole. Ground-based observations do not support this model (Smith and Sitko, 1991). However, new data recently published count in its favor. Thus, for the most actively observed blazar OJ 287 the model of a binary black hole with an accretion disk around the more massive component and jets from both components was developed. The large and variable polarization from some blazars observed in the visible is

associated with the dominant synchrotron emission in a jet. The reason for this is the flat wavelength dependence of polarization parameters in the optical region. Observations of several blazars with the HST (PKS 2155-304, OI 090.04, OJ 287) reveal that, though the degree of polarization is different in different objects, the absence of significant changes of polarization parameters with wavelength is typical for all of them (Allen et al., 1993; Smith et al., 1993b). Theoretical estimates show that the polarization may be higher in the accretion disk. For a better understanding of the nature of the polarization observed in blazars, data for the both optical and ultraviolet regions are necessary.

Quasars

A large list of bright quasars — about 270 objects — was proposed for observations with the HST (Bowen et al, 1994). Among quasars there are groups strongly distinguishing from each other by their flux characteristics in the radio and optical wavelength regions, for example, radioloud and radioquiet quasars, quasars with high and low levels of brightness variability, etc. For polarimetric observations with the HST the brightest objects with large redshifts, high optical polarization and brightness variability were selected. Several radiation mechanisms work in quasars: an optically thick thermal component which has its maximum intensity in the ultraviolet and a variable nonthermal partially polarized component. The degree of polarization of quasar emission in the ultraviolet is various in different models. The combination of polarization data in the optical region and in the ultraviolet allows us to determine polarization of each of these components. Thus, it facilitates the choice between different models. Therefore, spectropolarimetry with the HST gave the unique opportunity to find out which one of the different physical mechanisms is dominant.

The quasar 3C 273 has usually a small, about 0.5 %, polarization in the visible region. Observations with the HST showed a very small ultraviolet polarization. However, optical polarimetry points to the existence of a nonthermal component which is diluted by other sources of nonpolarized light, namely — a big blue bump. The analysis of observations reveals that the polarization of 3C 273 emission is not a result of dust or electron scattering (Smith et al., 1993a).

However, this is not a general rule. So, optical polarimetry of the quasar PG 1114+445 has shown that the polarization of forbidden lines is the same as the polarization of the continuum. It suggests that the polarization in this quasar is caused by the scattering of the light emitted from the nucleus by dust grains which exist outside the region where narrow emission lines are formed.

Another polarization picture is shown by the quasar OJ 287. As judged from the polarization spectrum of this quasar, the light emitted by the nucleus passes through a dusty environment, similarly to the light which is emitted by the nucleus of our Galaxy. Probably, this quasar is seen edge-on, and the sources of the continuous spectrum and the region of broad emissions are obscured by an optically thick but geometrically thin dust disk (Macchetto, 1994).

The quasar 3C 345 is a member of a small group of optically active quasars. Observations with the HST in two bands centered at 216 nm and 277 nm revealed a high polarization — more than 5 %. Unfortunately, no simultaneous ground-based observations were made. But such observations performed before and after the HST observations show that the parameters of ultraviolet and optical polarization are different even when possible changes with time are taken into account. This implies a difference between the characteristics of the quasar 3C 345 and Lacertides for which a less significant difference of polarization parameters in optics and in the ultraviolet is typical (Dolan et al., 1994).

In three quasars (PKS 0405-123, PG 1338+416, PG 1630+377) which were observed at wavelengths shorter than 300 nm (Kartatkar et al., 1995) changes of polarization along the spectrum are evident: the polarization near 200 nm is small — from 0 % to 4 % — and increases up to 20 % at 160 nm in PG 1630+377.

Ultraviolet spectropolarimetry was carried out for three bright quasars with large redshifts: PG 1222+228, PG 1634+706 and PG 2302+029 (Impey et al., 1995). Two of them (PG 1634+706 and PG 2302+029) have low polarization in the ultraviolet, about 0.5—1.0 %, which is practically independent of wavelength.

In the quasar with the largest redshift, PG 1222+228, the polarization is measured down to wavelength 80 nm in the rest system. The polarization of the continuum increased sharply from 1 % to about 4 %. Levels of ultraviolet polarization of these quasars are lower than in the visible. The energy distribution of polarized flux is described by a typical power-law index equal to -0.8 ± 0.5. The date obtained do not fit the model in which polarization arises due to scattering by dust as it is found in some galaxies of Seyfert 1 type. No decrease in polarization degree in the ultraviolet and no rotation of polarization plane predicted by some models were observed. In contrast, the increase in the degree of polarization observed in the ultraviolet in PG 1222+228 was so sharp that it

could not be caused by any mechanism giving a wavelength-independent polarization at any radius of the accretion disk around a black hole. So, the large growth in the degree of polarization can be caused by an increase of scattering rather than by absorption at high frequencies.

One can see from this brief review of published results obtained in the ultraviolet polarimetry of quasars with the HST that this group of objects is rather nonuniform in their polarimetric characteristics. Therefore, observations of quasars in the ultraviolet spectral region should be continued and as much objects as possible should be observed.

Jets

Ground-based observations revealed the existence of jets in many AGNs and quasars (galaxies M87, Cen A, PKS 0521-36, 3C 66B, 3C 273, etc.). The jet emission is strongly polarized and is of a synchrotron nature. The jets have complex structures, they consist of a number of knots of enhanced brightness and different sizes connected with each other. The extent of the jets does not exceed several arcseconds, and their widths are usually a fraction of arcsecond. So, the jet in the quasar 3C 273 is 25″ long. The jet images obtained in the ultraviolet spectral region with the HST allow the study of the fine structure of jets. The knowledge of polarization in the ultraviolet, optical, and radio regions allows one to determine the Faraday rotation of the plane of polarization and the magnetic field intensity in the jet and to study the interaction of the jet with its environment. These details are important for understanding the origin of the jets, their interaction with their environment, and the emission mechanisms in action in them.

3C 273 is one of the nearest quasars, and its jet has a relatively high surface brightness. A detailed polarimetric map of this jet was obtained by using the FOC at the HST (Thomson et al., 1993, Macchetto, 1994). The magnetic field structure appeared to be different at different locations in the jet, and the degree of polarization peaks up to 20 %. The data obtained do not support the assumption that the optical emission from the jet is simply the quasar light scattered toward the observer by grains in the jet. It is more probable that the radiation mechanism is the synchrotron emission of relativistic electrons in the magnetic field of the jet. A model proposed for the explanation of the jet phenomenon treats the jet as an ionized plasma ejected from the quasar into the environment. Study of the jet structure close to its outlet point led to the conclusion that the jet is unidirectional and is oriented almost perpendicular to the line of sight.

1.1.2. Stars

In the ultraviolet spectral region there are many spectral lines of different elements sensitive to physical parameters of stellar atmospheres. In this spectral region hot stars emit the maximum intensity of their radiation and a significant part of the emission is scattered by dust. Since the optical properties of the matter which the light has to pass through strongly vary along the spectrum, the comparison of data in the ultraviolet with data in optical and radio wavelength regions allows a number of important parameters to be determined, for example, the measure of Faraday rotation, magnetic field intensity, emission mechanism, source of scattering, structure of the dust envelope around the star, stellar wind, optical characteristics of grains, and the structure of their surfaces. Therefore, hot objects with well-developed ultraviolet spectrum are of particular interest: hot giants and supergiants, Be-stars, X-ray sources, Wolf-Rayet stars, white dwarfs, hot components of close binary systems, and nuclei of planetary nebulae. Up to now the following results of polarization studies of stars in the ultraviolet are published.

In 1990 spectropolarimetric observations of the red supergiant α Orionis with WUPPE in the wavelength region 150—330 nm and in the wavelength region 320—760 nm at the Pine Bluff Observatory were carried out. Analysis of data (Nordsieck et al., 1994) has shown that 1) there are at least two independent mechanisms of polarization with different geometry, working in different spectral regions; 2) the degree of polarization amounts up to 2 % at 300 nm and then rapidly decreases at 290 nm; 3) the emission line Mg II 280 nm is unpolarized. This suggests that the processes in the photosphere and chromosphere which are responsible for the polarization arise from the scattering of light in the atmosphere and/or in the dust envelope.

Important new results were obtained from observations of several Be-stars — emission stars with fast rotation. They are strongly variable, non-periodic, and show different characteristics in different wavelength regions. Variable stellar wind components are observed in the ultraviolet region. In the optical region a large (1—2 %) polarization of their radiation is observed. This fact, together with infrared excesses, the presence of lines belonging to an envelope, and the fast rotation, led to the conclusion that disk-like circumstellar envelopes exist around these stars.

Existing models of Be-stars predict an increase of the degree of polarization in the ultraviolet. However,

observations of some stars of this type — ζ Tau, φ Aqr and PP Car — made within the WUPPE do not confirm this prediction. On the contrary, constant or even decreasing degree of polarization in the continuum shortward of the Balmer jump and a wide region of lower polarization between 70 nm and 90 nm have been found. This phenomenon is explained by "dilution" of polarization due to the contribution from nonpolarized iron lines (Bjorkman et al., 1991, 1993).

Very important results were obtained from the study of three X-ray binaries: Cyg X-1 (HDE 226868), 4U 0900—40 (HD 77581), and 4U 1700—37 (HD 153919) (Wolinski et al., 1996). The ground-based polarimetry of these stars showed a small amplitude of their polarimetric variability. The wavelength dependence of polarization in the visible is well fitted by the Serkowski law for the interstellar polarization which dominates in the polarization observed in these stars. However, the wavelength dependence of the polarimetric variability amplitude in the visible observed in 4U 1700—37 and Cyg X-1 led to the conclusion that Rayleigh scattering is the mechanism which produces the intrinsic polarization in these systems. The wavelength dependence in the visible in 4U 0900—40 is consistent with Thompson scattering alone. If Rayleigh scattering is the principal mechanism producing the intrinsic polarization in these systems, the amplitude of polarimetric variability should be proportional to λ^{-4}, where λ is the wavelength. The Rayleigh scattering model predicts in this case that the amplitude of polarimetric variability should be greater in the ultraviolet than in the visible. These assumptions can be tested only by polarimetric measurements in the ultraviolet.

In fact, such observations made with HST in 1993 in five bands with central wavelengths 216, 237, 248, 277, 327 nm confirmed these assumptions. So, the amplitude of polarimetric variability in the UV in these stars is a factor of 20—30 greater than in the visible. The wavelength dependence in all three sources can be represented by a combination of the Rayleigh scattering component and a wavelength-independent Thomson scattering component. It follows from this model that the position angle of mean polarization is expected to rotate from the visible to the UV in the same way as the relative contribution of different components to the total polarization is changing from the visible to the UV. The smooth rotation of the position angle from the optical to the UV is consistent with the existence of a scattering component in each system, its contribution to the total polarization increasing in the UV relative to the amount of interstellar polarization.

While studying a peculiar Be-star with infrared excess, HD 45677, with WUPPE in the wavelength region 140—322 nm and in ground-based observations in the optical region (Schulte-Ladbeck et al., 1992b), a strong increase in the degree of polarization toward the shortwave region was found. It points to light scattering in a circumstellar dust envelope. A rotation of the plane of polarization by 90° in the near ultraviolet is due to the fact that the star is located in a bipolar reflection nebula.

Wolf—Rayet stars are of special interest because they have extremely strong stellar winds. Ground-based observations suggest that the geometry of mass loss is asymmetric in these stars. Therefore, polarimetry can give information on the structure of their stellar winds and emission mechanisms. Observations in the ultraviolet are of particular interest, as the continuous radiation is formed in denser parts of stellar winds, and ultraviolet emission lines are formed in regions quite different from those where optical lines are formed. Polarimetric observations of two such stars of different subclasses EZ CMa (WN5) and θ Mus (WC6 O9.5 I) gave distinct results. The ultraviolet polarization of radiation from EZ CMa appeared on a level of 0.8 %. Polarization features correspond to emission lines, and the large amount of polarization is indicative of a strongly asymmetric stellar wind, while in θ Mus the line polarization and the continuum polarization are equal and strongly decrease toward shorter wavelengths. The combination of ultraviolet and ground-based polarimetric data shows a wavelength dependence of polarization which is typical of the interstellar material, it is described by the Serkowski law (Schulte-Ladbeck et al., 1992a).

The HST observations of AG Carina, a prototype of the class of bright blue variable stars, during its flare phase show an intrinsic polarization of its radiation (Leitherer et al., 1994). It is considered as an evidence for the existence of a variable flow of matter, with its density increasing in the equatorial plane. Analysis of the star's spectrum revealed two stellar wind components, a slow one and a fast one, the latter having a smaller density. Analysis of the data showed that the temperature of this star had decreased from 21000 K to 14000 K in one year and its radius had increased by a factor of two. However, despite the significant changes in the photospheric conditions, the mass loss rate did not increase during these flares.

Despite of intensive studies of the properties of hot supergiants, many uncertainties still remain in our understanding of their mass loss mechanism. Mass loss rates in hot supergiants are second only to those in the Wolf—Rayet stars. It is clear from ground-

based observations that stellar winds from these stars are very nonuniform and asymmetric. Theoretical models predict a gradual growth of the degree of polarization in the ultraviolet and a decrease of polarization in Balmer lines. However, observations in the WUPPE and simultaneous ground-based observations of the hot supergiants P Cyg and κ Cas showed that the intrinsic polarization in the Balmer emission continuum in P Cyg was the same as outside it, except for a wide band between 260 nm and 300 nm as it is in typical Be-stars in the wavelength region at 200 nm. This drop in polarization supposed to be caused by blanketing of nonpolarized iron lines, just as this occurs in Be-stars. The intrinsic polarization is small in κ Cas, and the observed polarization is mainly interstellar, though there is some polarization excess in the ultraviolet as compared to models (Taylor et al., 1991).

1.1.3. Interstellar and intergalactic media

The interstellar matter may be considered in two aspects: as an obstacle in studying stars and galaxies and as an object in itself to be studied.

The major information about properties of the interstellar dust was obtained from observations in the optical and radio ranges. However, these data are insufficient to enhance our knowledge of physical characteristics of the dust. The optical properties of interstellar grains are known to vary strongly with wavelength, which results in the shape of the observed wavelength dependence of polarization and absorption. Essential changes in the characteristics of interstellar polarization are expected in the ultraviolet spectral region due to a sharp change of optical constants of dust grains. Therefore, for the determination of main characteristics of interstellar grains it is necessary to know the spectral variability of polarization in a wavelength region as wide as possible (Webb et al., 1993). This is important for the diagnostics of the chemical structure of cosmic dust in different regions of our Galaxy.

Even the first trial extra-atmospheric polarimetric measurements in two stars, β Ori and κ Cas, that were carried out in 1968 by Gehrels in bands centered at 225 nm and 286 nm confirmed the expected drop in the degree of polarization toward the ultraviolet end of the spectrum caused by the interstellar dust. More detailed data were obtained in the course of the Wisconsin project and with the HST in the wavelength region 130—300 nm (Clayton et al., 1992; Hanson et al., 1994; Taylor et al., 1991; Martin, 1994; Schulte-Ladbeck et al., 1992a, 1992b; Sommerville et al., 1994; Whittet et al., 1994; Wolff et al., 1993). Stars with their polarization known from ground-based observations — α Cam, HD 7252, 25443, 37903, 62542, 99264, 161056, 197770 — were observed. A strong rise in the degree of the linear polarization produced by the scattering of light by interstellar grains oriented in the galactic magnetic field was found in the ultraviolet region. Thus the intrinsic polarization can be detected in a number of astrophysical objects. A possibility to measure polarization at much shorter wavelengths will open a new way in analysing geometrical and optical parameters of small-sized dust grains.

By now the interstellar polarization in the ultraviolet was measured for 10 stars lying in different directions in the Galaxy. For 5 of these stars the spectrum of polarization is described by the Serkowski law, in 4 stars the polarization exceeds the amount expected, and only in one star (HD 197770) a polarization feature was found in the bump region on the curve of interstellar absorption at 217.5 nm (Anderson, 1994; Hanson et al., 1994; Martin, 1994; Whittet et al., 1994; Sommerville et al., 1994), the nature of the feature is not clear yet. It is supposed to be due to small oriented graphite disks (Wolff et al., 1993). The data obtained impose restrictions on the choice of a possible model for this feature on the interstellar absorption curve.

1.2. Scientific problems which can be solved only by the UVSPEPOL experiment

The above review of the polarimetric investigations in the ultraviolet which have been already performed or are planned for the near future allows us to conclude that only some first steps in development of this field have been made by now. The results obtained confirm an urgent necessity of continuing these studies. On the other hand, these results are not numerous, so there is a wide field of activity for the future research, in particular, this is a task for the observatory SPECTRUM-UV which will be the only space observatory working in this UV region in the next decades. Due to its large mirror and a convenient orbit, it would be possible to make a next great step in the UV polarimetry of cosmic objects.

We can offer the following problems as a preliminary program for polarimetric research on the T-170.

1.2.1. Extragalactic objects

Blazars

For blazars the main task is to study their variability in the UV region and to compare the results with the data obtained in the optical region. This can be done by accumulating long — 50—100 days — sets of observations of selected objects with good time coverage. Besides, it will be necessary to study the variability of polarization on a short time scale in continuous observations with a duration of about one day. The UVSPEPOL project is ideally suitable for this purpose, and we expect great improvements as compared to the HST observations. The data on polarization must be supplemented by photometric and/or spectrophotometric information, just as this requisite for other variable objects. The priority objects are OJ 287, PKS 0735+178, S5 0716+71.

Quasars

The main task for the UV polarimetry of quasars is to extend observations to the extreme UV region. (The extreme UV means normally 35 — 91.2 nm). This is rather important for the analysis of the nature of their emission in this wavelength range and for construction of appropriate models. It is desirable also to observe the quasars which are strongly variable and have a significant polarization in the visible (3C 279, 3C 345, 3C 66A) as well as the quasars with large redshifts.

1.2.2. Interacting close binary stars

The set of suitable objects is extremely large and includes stars of various nature — from supernovae to dwarf novae and many others, and so we have to restrict ourselves by selecting a small subset of objects which are of the prime interest for the UV polarimetry.

X-ray binaries

The most interesting objects are SS 433, Cyg X-1, and X-ray transient sources. For SS 433 there exist unpublished data obtained with the HST which show a high polarization (up to 15—20 %) in the UV. For Cyg X-1 and transients containing Be-stars it is difficult to separate intrinsic and interstellar polarization by using optical ground-based observations only. In the UV region, where the interstellar polarization is essentially smaller and the intrinsic polarization is predicted to be rather large, it will be possible to separate these two effects with greater certainty.

Magnetic interacting binaries — polars

Measurements of circular and linear polarization are the key tool for understanding the nature, geometry, and evolution of polars — of classic synchronized AM Her type stars as well as of intermediate non-synchronized systems. Observations in the UV region will provide new information which is very important for the construction of adequate models for these objects. Of special interest are UV observations of a new class of polars with magnetic fields of more than 100 megagauss for which the polarized harmonics of cyclotron radiation fall in the UV region. However, up to now no polarimetric UV data of any of these objects exist. To study polars, it is necessary to make continuous observations with a duration on the order of their orbital periods — from 1.5 to 6 hours — and with a time resolution on the order of several minutes.

1.2.3. Magnetic white dwarfs

Ground-based observations suggest that the majority of stars of this type have a complex spectrum with circular and linear polarization. At the moment it is not possible to describe this complex behaviour with suitable models. The extension of the observation region into the UV should help to construct more general model atmospheres for these stars and to clarify the geometry of their magnetic fields.

1.2.4. Interstellar polarization of distant reddened stars

The study of the interstellar polarization in various parts of our Galaxy in the UV region is of importance for both the research of the interstellar dust characteristics and adequate analysis of polarimetric observations of distant galactic objects with the aim to separate the interstellar local component in them. Preliminary results from the observations of interstellar polarization carried out with the HST clearly show that the wavelength dependence of this polarization cannot be always fitted by the extrapolation to the UV region of the well-known Serkowski law for interstellar polarization.

In addition to these particular observation programs, it is necessary to assess experimentally possibilities for solving new problems. We can point out two such problems.

Polarized proton and nuclear (He) cyclotron emission lines from accreting neutron stars with strong magnetic fields (10^{11}—10^{12} gauss) can be found only

in the ultraviolet region. Observations of these lines offer us a new method of direct diagnostics of the proton and nuclear components in the accreting plasma of neutron stars as well as a new method for the measurement of magnetic fields in neutron stars.

The UV polarimetry is an efficient method of a new field in astronomy — cosmic microphysics, which involves the development of astronomical methods for the search of new elementary particles— axions which are predicted by the modern physical theory of Great Unification and which can be a component of the hidden mass in the Universe. Such astronomical methods can be based on a new physical mechanism for the generation of polarized emission as a result of transformation of photons into axions and vice versa in the presence of a magnetic field, the so-called magnetic conversion. The most effective process is the magnetic conversion of photons in massless axions, the efficiency growing with photon energy. Possible observational evidence of this effect consists in:

1) the excess interstellar polarization of halo stars in the UV;

2) the excess polarization of the UV emission of distant quasars when their light is passing through galaxies with intermediate z;

3) the excess of intrinsic linear polarization of magnetic stars in the UV (see Gnedin and Krasnikov, 1992).

The wavelength dependence of polarization in the ultraviolet is quite strong. Therefore there is a necessity to make polarimetric observations in rather narrow spectral intervals which can be selected with the help of a set of filters. There is no need to separate narrow spectral lines, so the optimum decision seems to be a spectropolarimeter with low spectral resolution $R = 20—50$ and wavelength interval 115—365 nm. Various realizations of such a device are considered below.

PART 2.
GENERAL CONCEPT AND CHOICE OF A BASIC SYSTEM OF ULTRAVIOLET LOW-RESOLUTION SPECTROPOLARIMETER FOR THE SPECTRUM-UV EXPERIMENT

2.1. Equipment used in recent UV polarimetric observations

Only a few devices suitable for astrophysical ultraviolet polarimetric observations outside the Earth atmosphere have been developed up to now. These are the polarimeters for the Sun exploration (Stenflo et al., 1976; Gountail, 1978; Miller et al., 1981), HST polarimeters (Allen and Angel, 1982; Machetto et al., 1982; Bless et al., 1982; Lupie et al., 1988) and the spectropolarimeter of the Space Astronomy Laboratory of the University of Wisconsin (WUPPE) (Nordsieck et al., 1993a). While the solar polarimeters possess their own specific features related to the brightness of their observation object, the polarimetric instrumentation of the HST and WUPPE is close to the proposed UVSPEPOL project as regards the principles of design and scientific tasks.

2.1.1. Polarimetric facilities aboard the HST

When HST was designed, a concept was accepted according to which each instrument should have its own polarimetric unit. Such concept allows the optimization of polarizing optical components according to a particular observational task. There are three instruments aboard HST which have polarimetric modes for wavelengths below 300 nm. Those are Faint Object Spectrograph (FOS) (Allen and Angel, 1982), Faint Object Camera (FOC) (Machetto et al., 1982), and High-Speed Photometer (HSP) (Bless et al., 1982). Their characteristics are briefly described in Table 2 (Lupie and Stockman, 1988).

Table 2. Polarimetric Facilities of the HST Instruments

Instrument properties	HSP	FOC	FOS
Analyzer	4 UV-Polacoat	3 UV Double Rochons	Retarder/ Wollaston
Spectral range, nm	210 — 340	280 — 600	120 — 600
Polarimetric accuracy, %	0.2	1.0	0.1
Instrumental polarization, %	< 0.5	< 1.0	0.1
Target magnitudes	2 — 21 (stars)	21 sources > 16^m (extended)	> 9 (stars)

The Wide-Field and Planetary camera (WFPC2), in principle, also has a polarimetric mode for the near ultraviolet spectral range down to 220 nm, although its polarizing filters operate effectively only for $\lambda\lambda$ 300 — 650 nm. Besides, the WFPC2 polarimetric analyzer is followed by strongly oblique mirrors which

introduce an instrumental polarization of more than 6 % (Birctta et al., 1996).

The FOS spectropolarimeter

The FOS polarization module consists of two replaceable combinations of magnesium fluoride elements «retarder/Wollaston prism» located just after the entrance slit port. The mechanical mechanism has an original design and allows the rotation of the retarder with a 22.5-degree step and the input-output of the on-axis polarizing elements with a single motor. The retarders have different thickness, so they differ in their sensitivity to linear and circular polarization at different wavelengths. Both retarders together provide an adequate coverage of the FOS spectral range.

The Wollaston prism splits incoming light in two orthogonally polarized components, one of them is projected onto a multielement detector (digicon). The spatial separation of the two spectra formed by the optics of the spectrograph depends on the birefringency of magnesium fluoride at a given wavelength. It allows a separation of 780 μm at λ 153 nm, 242 μm at L_α, and the spectra merge at λ 117.5 nm.

Polarimetric analysis is performed by a conventional technique (Allen and Angel, 1982) based on the modulation of Stokes parameters by a rotating retardation element. For bright objects, the FOS polarimeter allows the measurement of the degree of polarization with an accuracy of 0.1 % and the position of the plane of linear polarization with an error of 0.5° in the spectral range 120 — 350 nm with a resolving power ≥ 250. However, the accuracy for faint objects is limited by the photon noise. A polarization error of 1 % is achieved during a 20-min exposure for a star of V = 15 mag, in a 10-nm bandwidth.

Recently, the polarimetric efficiency of the FOS has been slightly reduced owing to the installation of corrective optics (COSTAR) for the compensation of aberrations of the HST primary mirror. Two additional reflections introduce a 2 % wavelength-dependent instrumental polarization. Due to a number of reasons, only one of the two wave plates can be used. These restrictions impose a wavelength limit on polarization measurements at a wavelength of 165 nm and increase observational errors up to 0.2 — 0.7 % (Keys et al., 1995).

The FOC imaging polarimeter

The polarimeter configuration consists of three Double-Rochon type crystalline prism polarizers (Steinmetz et al., 1967) mounted in the filter wheel assembly of the $F/96$ optical relay. The optical axes of the outer wedges of each prism are oriented perpendicularly to the direction of propagation of the incident beam. The optical axis of the central prism component is parallel to the direction of beam propagation. The ordinary beam is transmitted without deviation and with minimum aberrations, while both extraordinary beams go separate ways after crossing the interface between the outer and central prism components. The angular separation of the beams is chosen so that the 512×512 pixel format in the central image area may be obtained without overlapping of the other orthogonally polarized beams. The main transmission planes of Rochon polarizers are located in angular directions of 0, 60, and 120 degrees, which secures complete analysis of linear polarization.

The prisms are assembled in optical contact, but the transmission of all three polarizers is different at wavelengths shorter than 300 nm. Moreover, one prism is completely opaque for wavelengths shorter than 180 nm.

Polarimetric accuracy (1σ) is 4—5 % for point sources and about 2 % for extended sources (Nota et al., 1996). The difference is basically caused by the fact that the point spread function (PSF) varies for different orientations of a thick anisotropic element (22.5 mm). The predicted instrumental polarization should be less than 1 %, but in practice it is rather difficult to measure this value as far as the effect is indistinguishable from that due to different prism transparency. Image shift due to switching of the prisms also creates additional problems in the analysis of the FOC polarimetric observations.

The HST photopolarimeter

The HST had a high-speed single-beam photopolarimeter mounted on a special filter/aperture assembly preceeding the Image Dissector Tube. The assembly panel consists of an array of four UV polarizers (3M Polacoat of 105 UV type) with transmission axes at 0, 90, 45, and 135 degrees followed by an array of four intermediate-band filters (30 — 40 nm FWHM) centered at wavelengths $\lambda\lambda$ 216, 237, 277, and 327 nm. Each filter/polarizer pair has a 1-arcsec diaphragm. Target pointing is executed by a small angular movement of the telescope.

One polarization data set is composed of four measurements with differently oriented polarizers and of four consecutive background measurements for stars fainter than U = 15 mag. The expected accuracy of the HSP was about 0.15—0.20 %.

The HSP instrument was removed from the HST instrumental section and was replaced by the corrective optical system COSTAR during the first HST

serving mission in 1993.

The HST observational technique and calibration procedure were discussed in details by Lupie and Stockman 1988; Nota et al., 1996; Keys at al., 1995.

2.1.2. Wisconsin spectropolarimeter WUPPE

The WUPPE instrument is a medium-resolution spectropolarimeter (1-nm resolution in spectral range 135—330 nm) assembled on the basis of a modified Monk — Gilleson spectrometer and equipped with the magnesium fluoride polarizing optics (Nordsieck et al., 1993a). The WUPPE was mainly designed for point targets and for polarization measurements of objects with high signal/noise ratio.

The polarization analyzer is located behind the entrance slit, it consists of sets of three pairs of magnesium fluoride half-wave retarders and of a magnesium fluoride Wollaston prism. The retarders are calculated for a phase shift of 180 degrees at λ 190 nm and consist of two 3-mm thick optically contacted layers with crossed optical axes. The Wollaston polarizer is 10 mm thick. All polarizing components are located in the convergent $F/10$ beam.

During polarization measurements the wheel containing retardation filters switches between waveplate orientations of 0, 45, 15, 60, 30, and 75 degrees. The Wollaston prism forms two spectra 25 mm long in the detector plane (two Reticon type photodiode arrays coupled to a single-stage ITT intensifier), they are separated by 3.5 mm. The pixel size along dispersion is 25 μm, which corresponds to 0.2 nm on the wavelength scale. The technique of polarimetric measurements used in the WUPPE was found to be weakly sensitive to guiding errors, gain changes in the detector, and noise events in the image tube. The overall system quantum efficiency is approximately 0.04, polarimetric efficiency is 0.75 (mainly due to the retarder's chromatism and small angular aperture), and the instrumental polarization (determined during the flight from observations of unpolarized stars) is less than 0.1 %.

As a matter of fact, the WUPPE design is similar to the arrangement of the HST FOS, however both beams leaving the Wollaston prism are used in WUPPE for polarization measurements.

2.2. Current engineering developments for UV polarimetric observations

Two new UV polarimeters are now under development in the Space Astronomy Laboratory of the University of Wisconsin. Those are a wide-field imaging polarimeter WISP (Wide-Field Imaging Survey Polarimeter) and a spectropolarimeter for the far ultraviolet spectral range FUSP (Far-Ultraviolet Spectropolarimeter). Nontraditional techniques for polarimetric analysis are applied in both instruments (Nordsieck et al., 1993b).

Imaging polarimeter WISP

The WISP instrument is intended for ultraviolet polarimetric investigation of diffuse objects with a field of view of 1.7×5 square degrees and a spatial resolution of 15 arcsec. The device will be used for an all-sky survey in two broad-band spectral intervals of 135 — 260 nm wavelength range during one-year mission. The advantage of the WISP experiment is that UV space observations of extended objects are completely free from most of the factors which complicate measurements and analysis of ground-based visible diffuse polarimetry (highly polarized variable background of the night sky, changes of atmospheric transparency, polarized zodiacal light background, unpolarized atomic emission from H II regions, and interfering radiation from foreground and background stars).

The Galactic reflection nebulae (Pleiades, NGC 7023, North America Nebula), diffuse clouds illuminated by distant stars (M81/82, Draco Cloud, Lockman Window), and some galaxies (LMC, M31) are chosen for the initial experiments with WISP. The prime tasks are the investigation of the optical properties of interstellar dust and the study of diffuse galactic light. In the UV region, only a small number of hot stars illuminate dust formations. So, by determining the angle of linear polarization, it will be possible to identify the sources of illumination and thus to study the 3-dimensional distribution of the Galactic dust and the 3-dimensional structure of other galaxies. Information about optical parameters of dust particles will be obtained simultaneously.

Structurally, the WISP is an integrated Schmidt telescope/polarimeter (diameter 19.5 cm, $F/9$) optimized for imaging polarimetric observations in the wavelength region 135—260 nm. The first device element is a very large retarder which consists of four 10×10 square cm plates made of an oriented calcium fluoride crystal. It is assembled in a special framework and attached, on two sides, to pneumatic actuators in order to get the desired phase shift by means of piezo-birefringency. The whole retarder mounting can be rotated. Any required phase retardation at a chosen wavelength can be achieved by controlling the force on the actuators. For the half-wave retardation at λ 200 nm the required force is

80 lbs per linear inch of edge.

The linear polarization Stokes parameters Q and U can be obtained by combination of the force and rotation of the calcium fluoride plate with the plate fixed at three angular positions (for Q-image, the angle is 45 degrees, the forces are zero and 80 lbs per linear inch; for U-image, the angles are 22.5 and 67.5 degrees, the force is 80 lbs per linear inch). The required force depends approximately linearly on wavelength.

It should be noticed that, with the polarization modulator located in front of the telescope, the instrumental polarization errors are excluded almost completely. Taking into account the excellent properties of a Schmidt telescope, this makes WISP a hundred thousand times more sensitive to diffuse light as compared to WUPPE.

A large 55×25 square cm rectangular flat Brewster angle plate coated by high-index monolayer of Y_2O_3 is used in the WISP as a polarizer. Several other materials with refractive indices from 2 to 3 at wavelength 175 nm are considered as alternative coating substances (Si_3N_4, La_5O_3, Nd_2O_3, ZrO_2, Ta_2O_5).

The detector is a Reticon RA 1200 CCD (400 × 1200 pixels with sides of 27 μm, thermoelectric cooling, 15 bit digitation). Primary and correcting Schmidt mirrors have the conventional $Al + MgF_2$ coating. Broad-band filters have central wavelengths of 164 and 218 nm and FWHM of 47 and 58 nm, respectively. The polarization modulation efficiency determined by retardation chromatism in the wide filter band does not drop below 70 %. Stray light and other background effects are minimized by superpolishing of all optical elements and by baffling.

The WISP has already flown successfully three times on a Terrier-Black Brandt sounding rocket: Dec 3, 1994 — Pleiades; Nov 20, 1995 — Large Magellanic Clouds (Nordsieck et al., 1996; Cole et al., 1997); Apr 7, 1997 — Comet Hale—Bopp. The next flight is scheduled for 1998 for the investigation of Galactic diffuse light targets.

Far ultraviolet spectropolarimeter FUSP

The spectropolarimeter FUSP is a natural extension of the WUPPE experiment into the far ultraviolet, where polarimetric data have never been obtained, although this is possible with polarizing optical transmission elements in the spectral range from 105 to 145 nm. This spectral range is of specific interest due to the presence of a number of strong resonance lines important for the diagnostics of stellar envelopes. Besides that, interstellar grains may change radically their optical properties in this wavelength range, which can be easily detect by polarimetry.

Rather bright objects, partially studied with WUPPE, were chosen as the first stellar targets for the FUSP mission. These are the bright Be stars γ Cas, ζ Tau, PP Car, white dwarfs γ Vel, EZ CMa, blue supergiant β Ori, as well as stars for testing the interstellar polarization — σ Sco, α Cam, P Oph, κ Cas.

The optical layout of the FUSP is as follows. The telescope has a primary mirror 40 cm in diameter and an angular aperture of $F/3$. The spectropolarimeter is mounted at the prime focus in an evacuated housing in order to avoid contamination of optical coatings and the detector. The telescope and spectropolarimeter mirrors will be LiF-coated aluminum.

The waveplate is made of lithium fluoride and serves as the spectrometer box window. The retarder measures 10×10×1 mm. Birefringency is produced by application of a force to the edge of the plate as in the WISP experiment, but the LiF retarder remains permanently in the stressed state. A pressure of 15 pounds is necessary to achieve half-wave retardation at λ 124 nm. A special strain gauge will monitor the strain and control the force required which can change owing to temperature variations, vibrations, and other processes. Phase modulation is executed by the retarder rotation through angles of 0 and 45 degrees (Q-spectrum) and 22.5 and 67.5 degrees (U-spectrum). A small diamond mirror at the Brewster angle at the prime focus of the telescope works as a polarizer.

A plane diffraction grating with 2400 grooves/mm provides a spectral resolution of 0.1 nm. Similarly to the WISP project, a CCD will be used as a detector. To achieve high polarimetric accuracy, short (approximately 10 sec) exposures are foreseen for each waveplate position. The CCD readout signal will be binned to 2×4 pixels in order to reduce the readout time to less than 1 sec. As the FUSP team estimates, for a flat-spectrum 0-magnitude star, with a spectral band of 0.1 nm at λ 120 nm, a 300-s exposure provides a polarimetric accuracy of 0.1 %.

The first FUSP flight is scheduled for the late 1998 on a 450-km orbit shuttle-deployed Small Explorer. The experiment is intended to look for magnetic fields in stellar envelopes using the Hanle effect (Ignace et al, 1997).

So, the HST polarimeters and the Wisconsin University instruments are the only instruments which provide information about ultraviolet polarization properties of stellar objects. Moreover, from all HST instruments only the FOS has sufficiently high polarimetric accuracy. However, during the second

Table 3. Stellar UV Polarimetric Experiments

Time	Experiment or author; mission or satellite	Telescope diameter, m; focal ratio	Spectral range or filters, nm	Largest exposure time, min	Polarization efficiency; polarimetric accuracy	Polarimetry	Objects
1966—1968	POLARISCOPE; balloon	0.71 *f*/13	220—285	short	$l = 1$; high	photo	2 stars
1972	GSFC; Aerobee rocket	0.33 *f*/10	120—400	short	$l = 1$; low	photo	1 star
1990	WUPPE; ASTRO-1	0.5; *f*/3	135—330	35	$l = (0.7—1.0)$; ordinary	spectral	20 bright galactic and extragalactic objects
1995	WUPPE; ASTRO-2	0.5; *f*/3	135—330	40	$l = (0.7—1.0)$; high	spectral	Comprehensive study of 244 various targets
1993—1997	FOS; HST	2.4; *f*/24	120—600	20	$l = (0.0—0.5)$; high $c = (0.0—0.5)$; high	spectral	Investigation of faint unique sources
1993—1997	FOC; HST	2.4; *f*/96	280—600	20	$l = 0.5$; low	imaging	Investigation of faint unique extended sources
1994, 1995, 1997, 1998	WISP; Terrier-Black Brandt sounding rocket	0.195; *f*/1.9	135—260	short	$l = (0.35—0.5)$; ordinary	imaging	Pleiades, Large Magellanic Cloud, Comet Halle-Bopp, diffuse objects
1998	FUSP; Small Explorer (450-km orbit)	0.4; *f*/3	105—145	~ 5	$l = (0.35\text{-}0.5)$; high	spectral	Stellar envelopes, interstellar medium
2000—2005	UVSPEPOL; SPECTRUM-UV	1.7; *f*/10	115—365	10000	$l = 0.8$; high $c = 0.8$; high	spectral, imaging	Long-term monitoring of faint unique objects

HST serving mission in February 1997, the FOS together with the Goddard High Resolution Spectrograph (GHRS) were replaced by two second-generation devices: the imaging spectrograph STIS (Space Telescope Imaging Spectrograph) and the infrared instrument NICMOS (Near Infrared Camera and Multi-Object Spectrometer) (Baum S. et al., 1996). These instruments, in principle, have no facilities for polarization experiments in the ultraviolet wavelength region. The FOC polarimeter, which remains the only large telescope device with polarization mode for wavelengths shorter than 300 nm, is of limited efficiency, as was stated above, due to its low accuracy of 4—5 %.

The Wisconsin experiments are run only episodically during short-term ASTRO missions, and small aperture telescopes are used. There will be no opportunity in the present state of affairs to measure circular polarization in the UV in the near future.

The proposed UVSPEPOL project enables us to measure simultaneously all four Stokes parameters in the vacuum ultraviolet. With such a powerful instrument as the T-170 telescope, it will be able to fill the gaps and overcome the limitations of the previous UV space experiments. The superiority of UVSPEPOL is clearly seen from Table 3, where previous, current and future stellar UV polarimetric experiments are listed. The polarization efficiency in this table is defined as $\sin\tau$ for circular (c) polarization or $(1 - \cos\tau)/2$ for linear (l) polarization (τ is the waveplate retardation) multiplied by factor 0.5 for single-beam polarimeters or by factor 1.0 for polarimeters using polarization beam-splitters and both orthogonally polarized beams. Polarimetric accuracy is considered as high for typical errors smaller than 0.1 %, ordinary for errors between 0.1 and 1.0 %, and low for errors larger than 1 %.

In addition, a number of novel technical solutions described in the following chapter will make the instrument unique and competitive for a decade ahead.

PART 3.
POSSIBLE STRUCTUR OF UVSPEPOL

3.1. General concept of the spectropolarimeter UVSPEPOL

Taking into account the experience of the polarimetric observations realized and considering the above-mentioned tasks, it is possible to formulate the main requirements to the polarimeter in the instrumental section of the Space T-170 Telescope:

1. The spectropolarimeter should be an independent instrument with its own panoramic detector.

2. It is preferable to fabricate polarizing optics from magnesium fluoride, which provides a polarimetric spectral coverage from 115 to 365 nm.

3. The polarimeter should have a facility to record all four Stokes parameters of ultraviolet radiation.

4. It is clear from the astrophysical tasks listed in Part 1 that the priority should be given to stellar objects of small angular size. Polarimetry of extended objects will be done in a separate auxiliary channel which can be used simultaneously for spectropolarimeter coordinate reference and guiding.

5. Since the central part of the focal plane of the T-170 telescope is occupied by the Field Camera, the polarimeter has to be designed for operating at some distance from the telescope's optical axis.

6. The spectropolarimeter should have maximum transparency and efficiency to measure faint objects.

An original and simple autonomous point-object spectral polarization analyzer will be described below. The layout and composition of the device proposed are fundamentally different from the conventional spectropolarimeters used before in space investigations, while the polarization characteristics of our instrument are much better than polarimetric facilities of previous on-board devices.

The instrument is based on two original ideas which make it superior in comparison with previous UV spectropolarimeters.

1. For the first time in the practice of spectropolarimetric measurements this instrument does not need any specialized dispersive elements and spectrograph optics. The dispersive functions will be provided by a Wollaston prism of original design consisting of two optically contacted wedges with spherical surfaces and displaced centers of curvature. The same prism serves also as a polarizing beam-splitter, just as in conventional polarimeters. Combination of imaging, dispersive, and polarizing functions in a single optical element increases the transmission of the optics three to ten times, which is especially beneficial for the ultraviolet region of the spectrum.

2. For the first time in the practice of ultraviolet polarization measurements we propose to use a unique ultraviolet achromatic retarder (AR) for the phase modulation of polarized light (Kucherov, 1996). It will improve the efficiency of polarization analysis of both linear and circular polarization in parallel for the whole UVSPEPOL operating wavelength range. Furthermore, there is no need to replace the modulators depending on different spectral ranges and different polarization types. This replacement is a disadvantage of other experiments, for example, in the FOS spectropolarimeter (Allen and Angel, 1982).

It must be noticed that visual achromatic elements of similar design (Kucherov et al., 1986) have been successfully used in major observatories in Russia (Special Astrophys. Obs., Central Astron. Obs. of RAS, Siberian Inst. of Terrestrial Magnetism, Ionosphere and Radio-Wave Propagation), Ukraine (Crimean Astrophys. Obs., Main Astron. Obs. of NAS), Georgia (Abastumani Astrophys. Obs.), as well as in many Ukrainian scientific institutes and industrial plants.

The spectropolarimeter will consist of only two optical components, which provides its compactness, relative cheapness, and high efficiency. Polarization modulation will be performed by step rotation of achromatic retarder with a phase shift of about 127 degrees, providing the same sensitivity of the system to both the linear and circular polarization of radiation. A special Wollaston prism will project two orthogonally polarized spectra from point sources onto a panoramic detector. The geometric characteristics of the location of the spectra in the detector plane, the form and scale of dispersion, and the degree of aberration distortions (including those from the telescope optics) can be regulated by appropriate choice of prism design parameters. The preliminary stage in the design of the special Wollaston prism is described elsewhere (Kucherov et al., 1995; Ivanov and Ivanov, 1997, in preparation).

Structurally the polarimeter will consist of two channels located at a distance of 80—100 mm from the optical axis of the T-170 telescope above the Double High-Resolution Spectrograph. The principal spectral channel will consist of AR, Wollaston prism, and an auxiliary oblique mirror inserted for a convenient detector location. The additional tracking and imaging polarimetry channel will include AR, Brewster reflection polarizer, and spectral filters, if

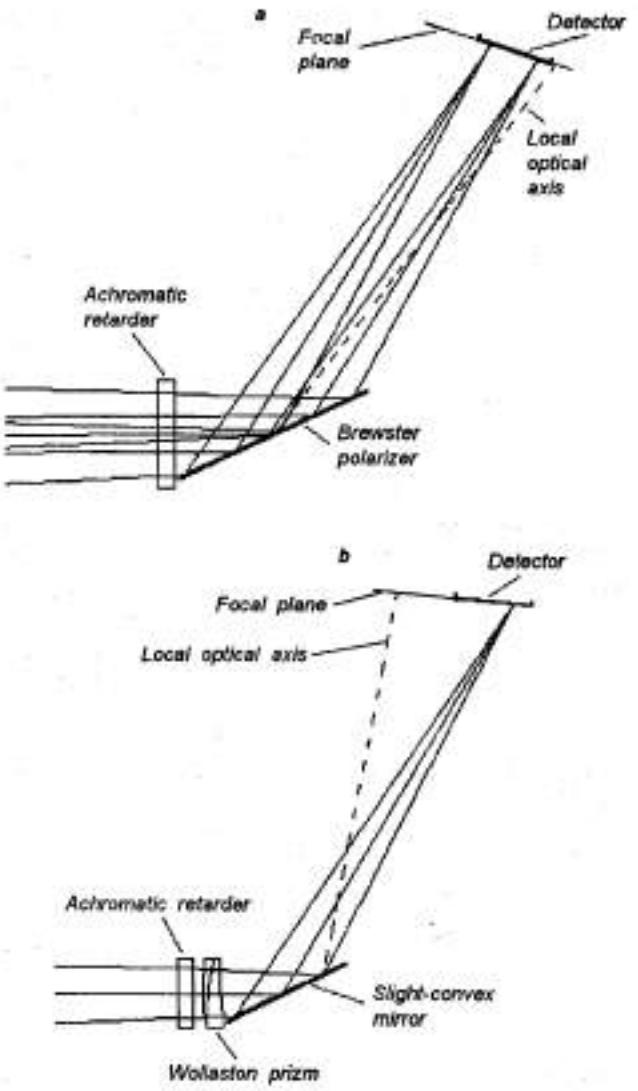

Fig. 1. *a*) Schematic diagram for the imaging polarimeter; *b*) Schematic diagram for the spectropolarimeter

necessary. ARs in both channels will be rotated by the same motor. Provision is made for each channel to have its own independent panoramic detector. Preliminary schematic diagrams of the both channels are shown in Fig. 1. The resulting thickness of the transmission optics will not exceed 10 mm.

Various aspects of the device connected with the instrumental polarization problems and Brewster polarizer design have been considered in detail by Kucherov (Kucherov et al., 1995). Below we dwell only on the principal functional elements of the UVSPEPOL spectral channel.

3.2. Ultraviolet achromatic phase retarder

Achromatic polarization phase modulators have never been used till now in the ultraviolet spectral region. The reason is that there are no suitable materials for polarizing optics for the use in the ultraviolet, and appropriate theoretical studies in this special field were also lacking. At the same time we know from the experience of visible polarimetric observations that the use of ARs is most promising in spectropolarimetry.

We have developed for the first time a vacuum ultraviolet achromatic retarder (Kucherov, 1996a) and we propose to use such an element in the UVSPEPOL experiment. The proposed AR is a multicomponent retardation system with appropriate thicknesses and optical axis orientations of crystalline layers. The structural parameters of such a system are chosen to meet self-compensation conditions, namely: the equivalent system phase shift and the equivalent optical axis position should not change when phase shifts of the individual components deviate from their nominal values when, for example, wavelength changes. An example of the achromatization properties of such an AR made of 10 optically contacted magnesium fluoride monocrystalline layers is shown in Fig. 2 (magnesium fluoride is the only material for phase plate fabrication in the wavelength range below 200 nm). For comparison a part of the spectral dependence of phase shift for one of the FOS polarimeter phase plates is shown in the same figure (the left-hand branch of the latter curve corresponds to anomalous dispersion of magnesium fluoride birefringence). By comparing these curves one can conclude that the element chosen for UVSPEPOL is much superior to the HST FOS phase plate. It should be emphasized that anomalous dispersion of MgF_2 birefringence at wavelengths shorter than 130 nm expands the spectral range of achromatization in our synthesis technique and gives rise to a small additional operating zone at $\lambda\lambda$ 116—118 nm, where magnesium fluoride crystal is transformed from positive to negative one. On the whole, the phase shift deviation over the spectral interval from 122 to 300 nm does not exceed 2.5 degrees, while the position of the optical axis does not change by more than 0.75 degrees; such polarization behaviour is considered good even for the visible spectrum. If the tolerance to be accepted is two times worse, the system will be successfully optimized in the spectral range from 122 to 500 nm.

One obstacle in the realization of our approach may be the manufacturing of such a complex multicomponent AR. Therefore, as an alternative, we propose a multiachromatic retarder (MAR) with half as many components. Such an element is achromatic only in a

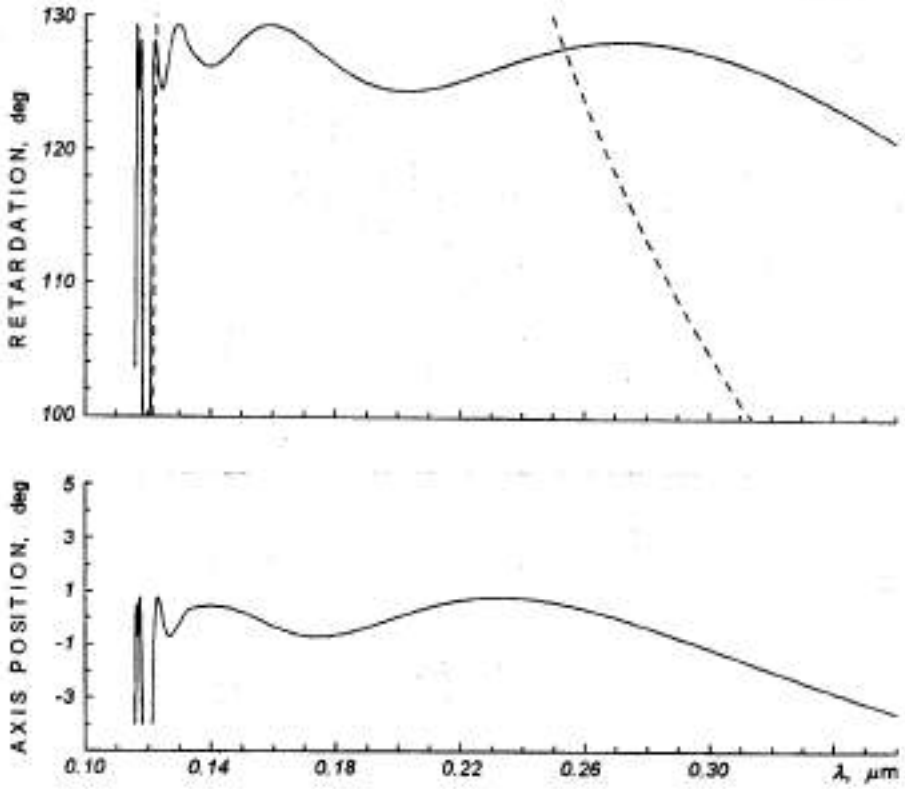

Fig. 2. Spectral properties of a 127-degree achromatic retarder. Dashed line represents the phase shift of the HST FOS polarimeter phase plate

part of the spectral range of a given order of interference. Nevertheless, the theoretical principles of its operation are the same as for the AR described above. The advantage of MAR is that it has no limitation over a wide spectral range — it can operate from λ 114 nm to λ 7000 nm.

However, the information capacity of MAR will be 2—3 times lower because of gap-achromatic spectral function of the element. Outside the achromatic zone light suppression, a Solc-type birefringent filter having a structure similar to MAR and differing only by axis orientations of the components can be used (Kucherov, 1996i). But if the wavelength scale is correctly referred to detector pixels and target tracking is reliable, there is no need to use any filters in this spectropolarimeter as far as the reduction of observations can be performed only for achromatized zones.

An example of MAR calculation (solid line, the scale is on the left) accompanied by matching filter (dashed line, the scale is on the right) is displayed in Fig. 3 for three different wavelength regions. A 106-degree phase shift was chosen as an optimum for the given type of element as a result of the theory of multicomponent retardation system synthesis. In the example the MAR and the Solc filter consist of 5 components of magnesium fluoride, each component being approximately 0.5 mm thick.

One further problem in the application of the UV AR is a strong sensitivity of its phase shift to oblique rays. Estimation of this factor seems to be a rather complex task, and it may require special ray-tracing software having polarization/anisotropic media modes. Our preliminary study of composite waveplates in the visible spectral region and estimations made for the double thick WUPPE UV retarders (Nordsieck et al., 1993a) show that the retardation of UV AR is not seriously reduced in the convergent $f/10$ T-170 beam.

3.3. Results of aberration calculations of polarimetric units

The following factors should be taken into consideration when optical systems are calculated for polarimetric units:

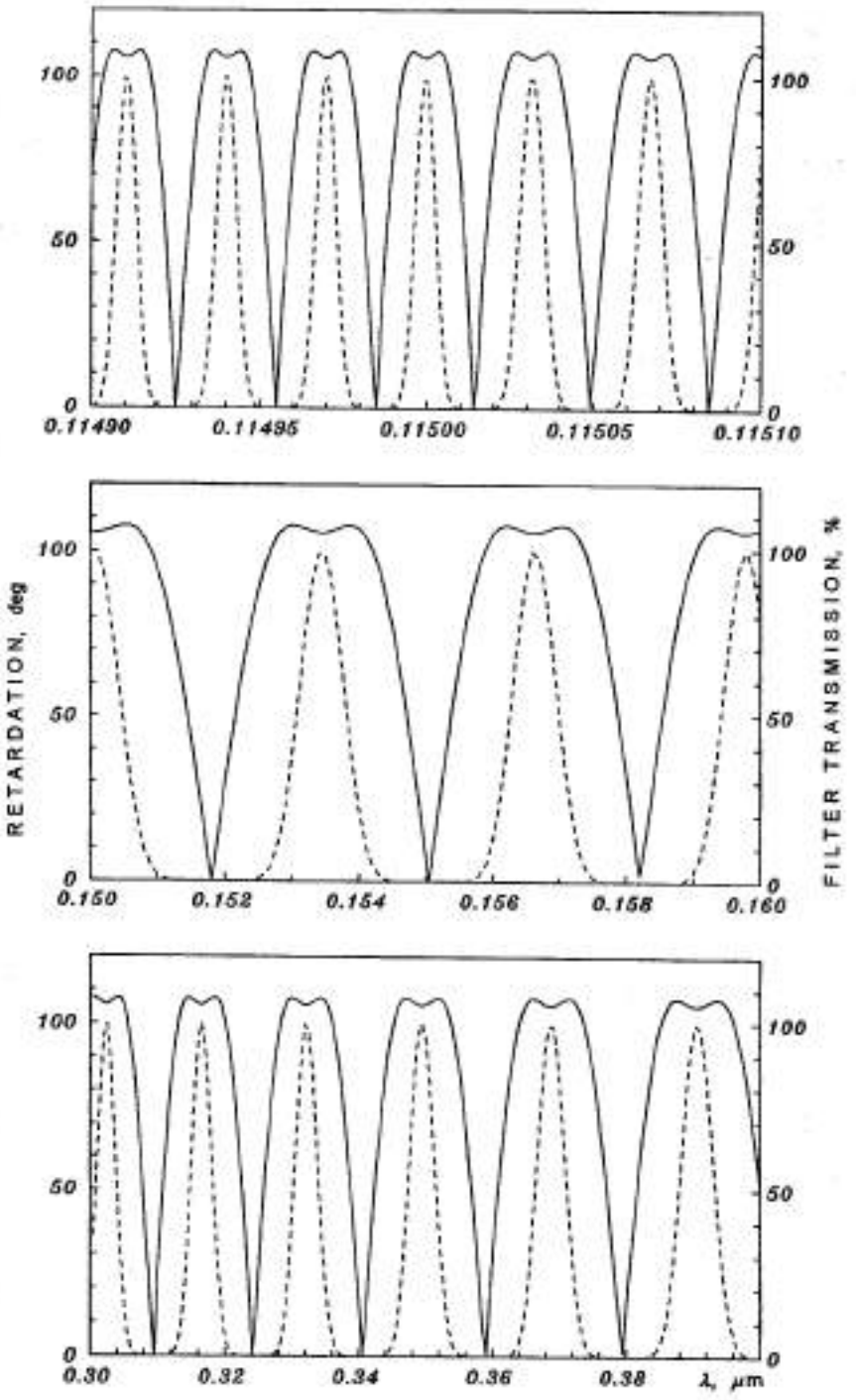

Fig. 3. Spectral properties of a multiachromatic retarder in three spectral regions

1. Magnesium fluoride, which is the only transparent material operating in the required spectral range, has a reduced transmission for wavelengths shorter than 200 nm. To increase the limiting magnitude for this telescope, the number of elements as well as their thickness should be minimized.

2. The off-axis astigmatism of the polarimetric units, which is the dominating image aberration,

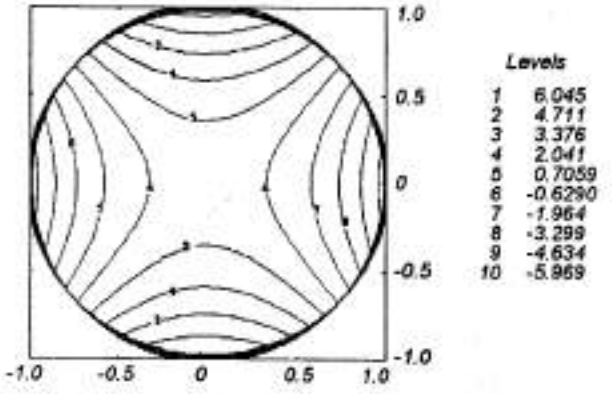

Fig. 4. Wave aberrations in the imaging polarimeter (in wavelengths) for λ 126.5 nm. Initial variant

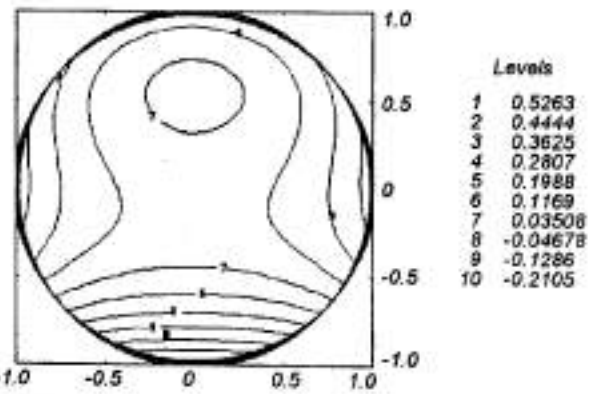

Fig. 5. The same as in Fig. 4 after correction

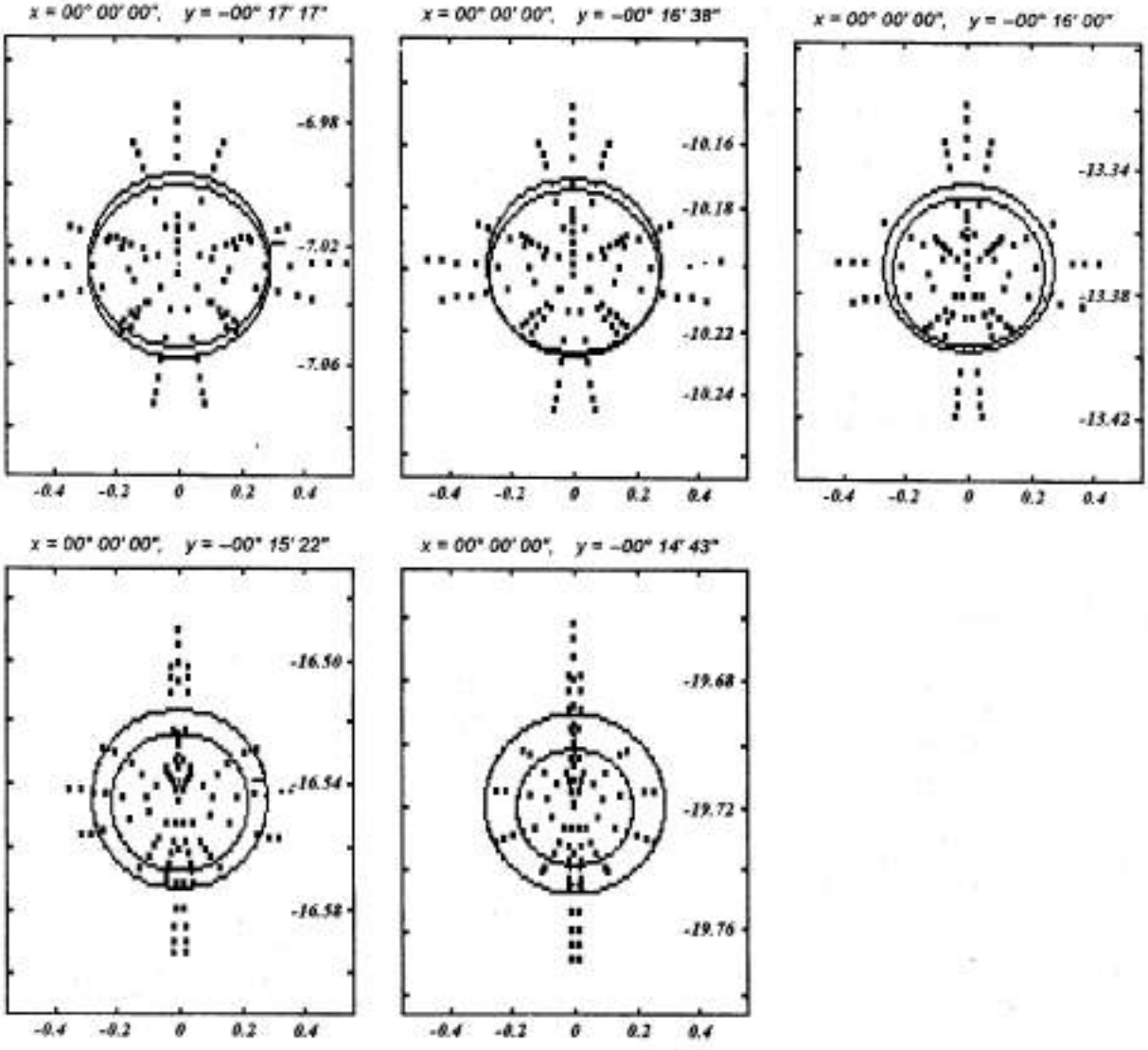

Fig. 6. Spot diagrams in the meridional plane for the imaging polarimeter for $\lambda\lambda$ 126.5 and 365 nm. Initial variant. x, y are the angular coordinates of the incident beam. Scale is in mm. The circles correspond to a 80 % level of energy concentration

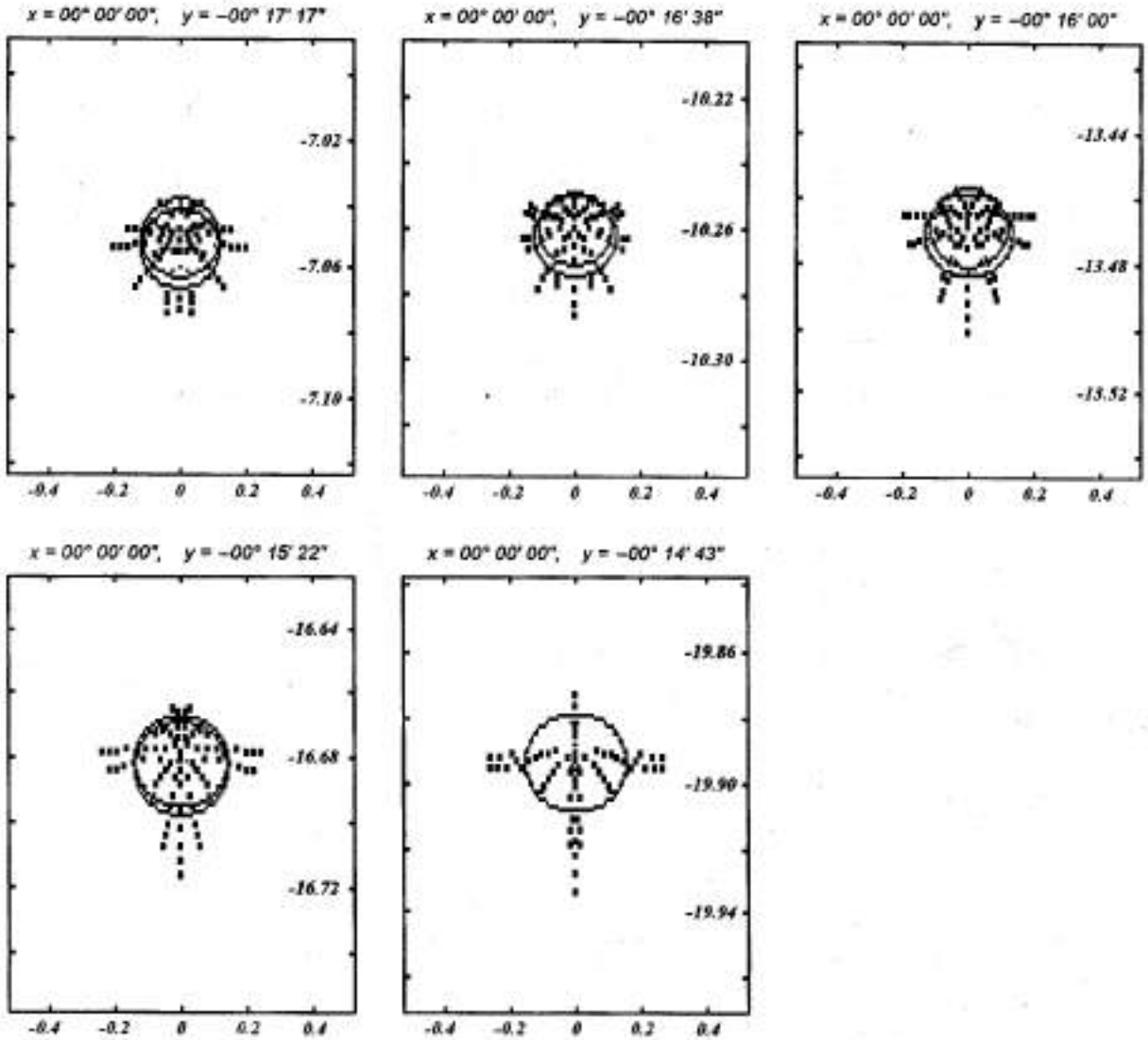

Fig. 7. The same as in Fig. 6 after correction

enlarges the point spread function up to 40—50 μm. To achieve a high limiting magnitude, this kind of aberration must be corrected (the PSF must not be broader than the detector pixel size).

3. A plane-parallel phase plate positioned in a convergent beam introduces all kinds of aberrations. These aberrations must be corrected as well.

From the arguments mentioned above, it is clear that each optical element in our system should perform the maximum number of power, polarizing, and corrective functions simultaneously. Due to the fact that there are only few free corrective parameters, their number should be increased artificially by introducing inclinations and displacements rather than by increasing the total number of elements. Preliminary calculations verified the fruitfulness of such an approach (Kucherov et al., 1995).

3.3.1. Tracking channel/imaging polarimeter

With a wide-band achromatic phase plate, we were able to choose the simplest layout which consists of two elements (retarder and polarizer) only. As a polarizer, a Brewster magnesium fluoride plate will be used (Fig. 1). It should be noticed that a technique exists with which diamond-like thin films are deposited on an arbitrary substrate. This variant

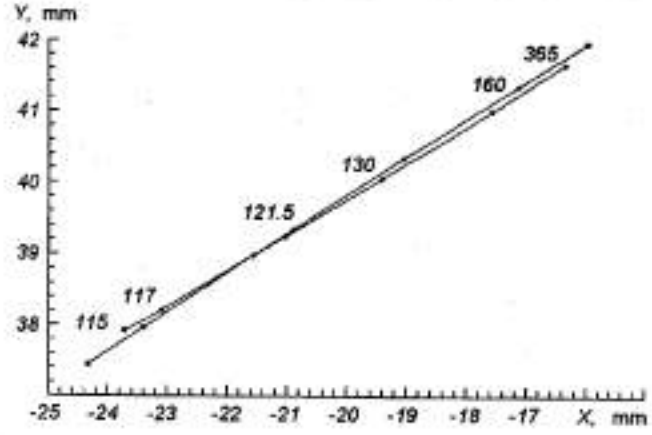

Fig. 8. Ordinary and extraordinary spectra built by the spectropolarimeter. Decenterings (positions in mm of the second and the third curvature centres of the Wollaston prism relative to the first one) are $Dx = -5$ mm, 15 mm; $Dy = -5$ mm, 10 mm. Relative compression is 3, 2

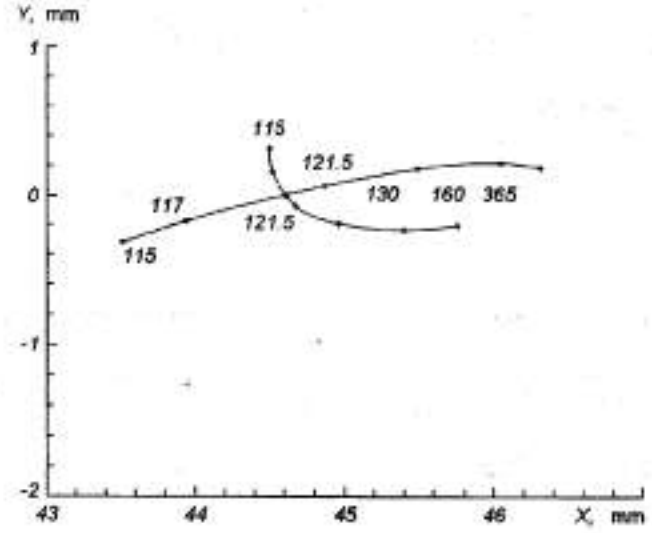

Fig. 9. The same as in Fig. 8. Decenterings are $Dx = -7.5$ mm, 15 mm; $Dy = -7.5$ mm, 10 mm. Relative compression is 4, 3

promises an increase in the device efficiency due to high refractive index of diamond (garnet, etc.) which slightly changes in a wide spectral band. This needs further investigation because no information is available about the optical characteristics of such thin films in the required spectral region.

The astigmatism and the weak coma introduced by phase plate are corrected by giving a small positive curvature to the surface of the polarizer. There is no way to compensate for the phase plate chromatism, but it can be minimized by tilting the plate by an

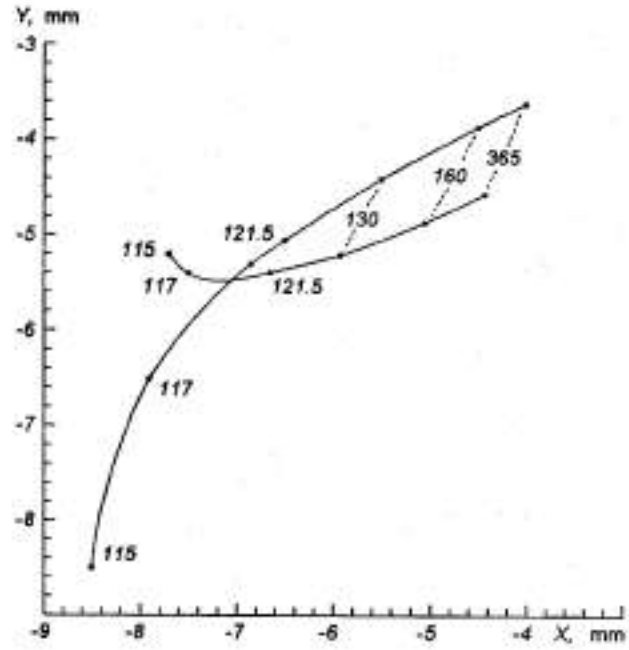

Fig. 10. The same as in Fig. 8. Decenterings are $Dx = -12.5$ mm, 15 mm; $Dy = -10$ mm, 10 mm. Relative compression is 7, 8

angle of −40 arcmin and by oblique ray incidence on the detector.

Successfulness of the method proposed by us is illustrated by the wave—aberration plots calculated before (Fig. 4) and after (Fig. 5) correction. One can see that astigmatism is completely compensated and only a residual coma is still appreciable. On the whole, the aberration is reduced by almost an order of magnitude and the values typical for the center of the telescope's field of view have been reached.

Figures 6 and 7 present the corresponding spot diagrams. The rms dispersion diminished only by a factor of 3, which may be explained by an irremovable phase plate chromatism. However, the results which were obtained from preliminary calculations are quite convincing and there are further reserves for decreasing the PSF.

3.3.2. Spectropolarimeter

The spectropolarimeter arrangement can be obtained by adding a Wollaston prism to the system (Fig. 1). Naturally the system partially looses its panoramic imaging properties, and only point objects can be observed. However, much better aberration corrections can be achieved by some deformation and decentering of the prism surfaces.

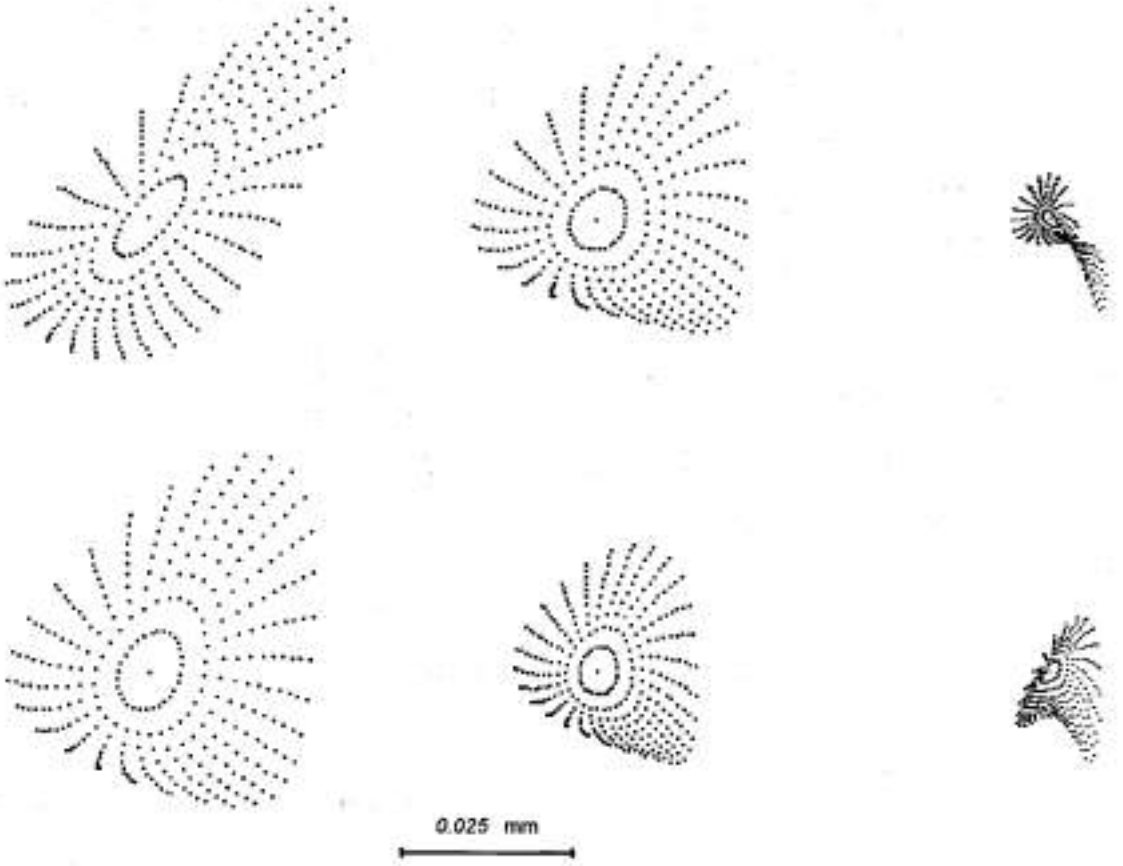

Fig. 11. Spot diagrams for the ordinary and extraordinary rays in the spectropolarimeter

Calculations show that the system, while extremely simple, is highly flexible and allows practically any desired dispersions, resolutions, and forms of spectra. At the same time it allows correction for the initial aberrations of the telescope. Examples are given in Figs 8—10. One can see that a significant dispersion compression at shorter wavelengths and compression extension at longer wavelengths, i. e., spectrum dispersion alignment, can be easily achieved for the extraordinary beam to a reasonable degree. This will increase the telescope's limiting magnitude. The corresponding gain (the dispersion ratio in blue rays of decentered and nondecentered variants of the Wollaston prism) is called "relative compression" in the figure captions. The decenterings are chosen such that both spectra may make angles of approximately 45 degrees with the principal axes of the polarizer to equalize the spurious polarization introduced by an auxiliary oblique mirror in the ordinary and extraordinary spectra.

Imaging quality for all given variants is much higher than the imaging quality of the imaging polarimeter unit. The initial astigmatism is corrected partially by a slightly convex mirror and partially by Wollaston prism inclinations, while the phase plate chromatism is compensated by deformations of the prism surfaces and detector plane inclination. Spot diagrams for ordinary and extraordinary rays are displayed in Fig. 11.

This figure and the corresponding calculations show that the PSF exceeds the detector pixel size only in the extreme ultraviolet spectral region.

Thus, preliminary calculations confirm the feasibility of obtaining high-quality polarization spectra with an arbitrary spectral resolution (up to several thousands) and with convenient locations of the spectra on the detector surface.

CONCLUSION

Detailed calculations have clearly demonstrated the possibility to create a high-transmission spectropolarimeter based on a novel technology (UVSPEPOL). The instrument has the following advantages:

1. For the next decade the UVSPEPOL will be the only polarization instrument operating with a large-aperture telescope and covering the ultraviolet spectral region.

2. Only UVSPEPOL will be able to measure all types of polarization over the whole UV spectral region (from vacuum to near UV).

3. Coupled to the Space Telescope T-170, the device will provide a unique limiting magnitude for polarization modes and will outperform the HST in this respect.

4. The instrument, while very efficient, is very compact, and its manufacturing cost is low.

5. The opportunity for effective compensation of aberrations allows an off-axis positioning of the instrument without interfering with other devices in the instrumental section.

6. Spectral observations can be accompanied by imaging observations, which will not only increase the amount of useful information but will also expand the functional facilities of the T-170 telescope as well (pointing, tracking, etc.)

Acknowledgement

Authors are very grateful to Dr. N. Kappelmann (Institute for Astronomy and Astrophysics, University of Tübingen, Germany) for his kindly help in preparation of this manuscript and very useful advice.

REFERENCES

Allen R. G., Angel J. R. P. Performance of the spectropolarimeter for the Space Telescope Faint Object Spectrograph // SPIE.—1982.—331.—P. 259—267.

Allen R. G. et al. Ultraviolet polarimetry and spectroscopy of the BL Lacertae object PKS 2155-304 // Astrophys. J.—1993.—403, N 2.—P. 610—620.

Anderson C. M. Optical interstellar absorption along WUPPE interstellar polarization sight lines // BAAS.—1994.—26, N 2.—P. 901.

Annual report of the Space Telescope Science Institute (October 1992—September 1993) // BAAS.—1994.—26, N 1.—P. 618.

Antonucci R. et al. HST ultraviolet spectropolarimetry of NGC1068 // Astrophys. J.—1994.—430, N 1.—P. 210—217.

Allen R. G. et al. Ultraviolet polarimetry and spectroscopy of the BL Lacertae object PKS 2155-304 // Astrophys. J.—1993.—403, N 2.—P. 610—620.

Baum S. et al. Space Telescope Imaging Spectrograph Instrument Handbook. Version 1.0. — Baltimore: Space Telescope Science Institute, 1996.

Biretta J. et al. Wide Field and Planetary Camera 2 Instrument Handbook. Version 4.0. — Baltimore: Space Telescope Science Institute, 1996.

Bjorkman K. S. et al. First spectropolarimetry of Be stars from the Wisconsin Ultraviolet Photo-Polarimeter Experiment // Astrophys. J.—1991.—383, N 2.—P. L67—L70.

Bjorkman K. S. et al. Ultraviolet spectropolarimetry of the Be star PP Carinae with the Wisconsin Ultraviolet Photo-Polarimeter Experiment // Astrophys. J.—1993.—412, N 2.—P. 810—813.

Bless R. S. et al. The High Speed Photometer for the Space Telescope. The Space Telescope Observatory, Baltimore, Space Telescope Sci. Institute, 1982.—P. 106—113.

Bowen D. V. et al. Hubble Space Telescope Faint Object Spectrograph Quasar Absorption System Snapshot Survey (ABSNAP). I. Astrometric optical positions and finding charts of 269 bright QSOs // Astron. J.—1994.—107, N 2.—P. 461—465.

Boyarchuk A. A., Tanzi E. G. SPECTRUM-UV Project // Mem. Soc. Astron. Ital.—1993.—64.—P. 263.

Calvert J. et al. An ultraviolet polarimeter for the Solar Maximum Mission // Opt. Eng.—18, N 3.—P. 287—290.

Capetti A. et al. HST polarization observations of NGC 1068 // BAAS.—1994.—26, N 2.—P. 957—958.

Capetti A. et al. HST imaging polarimetry of NGC 1068 // Astrophys. J.—1995.—446, N 1.—P. 155—166.

Clayton G. C. et al. The first spectropolarimetric study of the wavelength dependence of interstellar polarization in the ultraviolet // Astrophys. J.—1992.—385, N 2.—P. L53—L57.

Code A. D. et al. The first ultraviolet spectropolarimetric study of NGC 1068 // Astrophys. J.—1993.—403, N 2.—P. L63—L65.

Cole A., Nordsieck K. H., Gibson S. J, Harris W., Wood, 1997, BAAS, 190. 0205.

Dolan J. F. et al. The linear polarization of 3C 345 in the ultraviolet // Astrophys. J.—1994.—432, N 2.—P. 560—566.

Fineschi S. et al. Polarimetry of extreme ultraviolet lines in solar astronomy // Opt. Eng.—1991.—30, N 8.—P. 1161— 1168.

Gehrels T. Wavelength dependence of polarization. XXVII. Interstellar polarization from 0.22 to 2.2 μm // Astron. J.—1974.—79, N 5.—P. 591—593.

Gershberg R. E., Zvereva A. M., Petrov P. P., et al. SPECTRUM-UV Cosmic Experiment Project // Kosmichna Nauka i Technologiya.—1995.—1, N 1.—P. 47—55 (in Russian).

Gnedin Yu. N. Scientific Programme for Polarimetric Observations Within the Framework of the SPECTRUM-UV Mission // SPECTRUM-UV Project Documents. — Kyiv: MAO RAS, March, 1996.

Gnedin Yu. N., Krasnikov S. V. Polarimetric effects related to the discovery of Goldstone bosons in stars and galaxies // JETPh.—1992.—102, N 6.—P. 1729—1738 (in Russian).

Gountail F. Polarization of the solar UV light at the limb // Astron. and Astrophys.—1978.—64, N 12.—P. 73—82.

Hanson M. M. et al. Carbon chemistry in the polarized 2175 A bump sightline toward HD 197770 // First Symposium on the Infrared Cirrus and Diffuse Interstellar Clouds. — 1994.—P. 84—87.

Hoover R. B. et al. Optical configurations of H Lyman alpha coronograph polarimeter // SPIE.—1991.—1546.—P. 414—431.

Hoover R. B. et al. Design and fabrication of the all-reflecting H-Lyman alpha coronagraph polarimeter // SPIE.—1992.—1742.—P. 439—452.

Hoover R. B. et al. Fabrication and test of a wide field Lyman alpha coronagraph polarimeter // SPIE.—1993.—2010.—P. 104—116.

Impey C. D. et al. Ultraviolet spectropolarimetry of high-redshift quasars with the Hubble Space Telescope // Astrophys. J.—1995.—440, N 1.—P. 80—90.

Ignace R., Nordsieck K. H., Cassinelli, J. P. The Hanle effect as a diagnostic of magnetic fields in stellar envelopes. I. Theoretical results for integrated line profiles // Astrophys. J.—1997.—486, N 1.—P. 550—570.

Ivanov Yu. S., Ivanov D. Yu. Imaging polarimeter with a Wollaston prism // 1997. (in press).

Keys C. D. et al. Faint Object Spectrograph Instrument Handbook. Version 6.0. Space Telescope Science Institute, Baltimore, 1995.

Koratkar A. et al. Quasar Lyman edge regions in polarized light // Astrophys. J.—1995.—450, N 2.—P. 501—507.

Kucherov V. A. et al. Achromatic Phase Plate. SU Author Certificate 1269067 // Invention Bull.—1986.—N 47 (in Russian).

Kucherov V. A. et al. Development of Main Principles of T-170 Polarimetric Unit Creation // SPECTRUM-UV Project Documents. — Kyiv: MAO NANU, 1995.

Kucherov V. A. Achromatic retarder for the vacuum ultraviolet // Kinematics and Physics of Celestial Bodies.—1996a.—12, N 1.—P. 52—58.

Kucherov V. A., Efimov Yu. S. On Polarimetric Observation in the Ultraviolet // SPECTRUM-UV Project Documents. — Kyiv, March, 1996.—1996b.

Kucherov V. A. A simple way for Solc filter synthesis // Kinematics and Physics of Celestial Bodies.—1996c.—12, N 1.—P. 59—70.

Leitherer et al. // Annual Report of the Space Telescope Science Institute.—1994.

Lupie O. L., Stockman H. S. Calibration of the Hubble Space Telescope polarimetric modes // Polarized Radiation of Circumstellar Origin / Eds G. V. Coyne at al. — Vatican Observatory — Vatican City State, 1988.—P. 705—726.

Macchetto F. at al. The Faint Object Camera // The Space Telescope Observatory. — Baltimore: Space Telescope Scientific Institute, 1982.—P. 40—54.

Macchetto F. Hubble Space Telescope observations of AGN // Multiwavelength Continuum Emission of AGN: IAU Symp. N 159 / Eds T. J.-L. Courvoisier and A. Blecha. — 1994.—P. 83—104.

Martin P. G. Polarization of the 2175 Å extinction feature // J. R. Astron. Soc. Canada.—1994.—88, N 4.—P. 266.

Miller M. S. et al. Ultraviolet spectrometer and polarimeter for the Solar Maximum Mission // Appl. Opt.—1981.—20, N 21.—P. 3805—3814.

Nordsieck K. H. et al. Exploring ultraviolet astronomical polarimetry: Results from the Wisconsin Ultraviolet Photo-Polarimeter Experiment (WUPPE) // SPIE.—1993a.—2010.—P. 2—11.

Nordsieck K. H. et al. New technique in ultraviolet astronomical polarimetry: wide-field imaging and far ultraviolet spectropolarimetry // SPIE.—1993b.—2010.—P. 28—36.

Nordsieck K. H. et al. Ultraviolet visible spectropolarimetry of alpha Orionis // BAAS.—1994.—26, N 2.—P. 864.

Nordsieck K. H. Cole A., Gibson S. J., Harris W. Polarimetric imaging of the ultraviolet diffuse light in the Large Magellanic Cloud // BAAS.—1996.—28, N 1.—P. 757.

Nota A. et. al. Faint Object Camera Instrument Handbook, Version 7.0, Space Telescope Science Institute, Baltimore, 1996

Pian E., Trevis A. The UV continua of blazars: a reconsideration of IUE archives // Astrophys. J.—1993.—416.—P. 130—136.

Schmidt G. D. et al. // Astron. J.—1992.—104, N 4.—P. 1563—1567.

Schulte-Ladbeck R. E. et al. The first linear polarization spectra of Wolf-Rayet stars in ultraviolet: EZ Canis Majoris and q Muscae // Astrophys. J.—1992a.—391, N 1.—P. L37—L40.

Schulte-Ladbeck R. E. et al. Evidence for a bipolar nebula around the peculiar B[e] star HD 45677 from ultraviolet spectropolarimetry // Astrophys. J.—1992b.—401, N 2.—P. L105—L108.

Serkowski K. Polarization techniques // Methods of Experimental Physics. Astrophysics. — New York—London: Acad. Press, 1974.—Pt. A.—P. 361—414.

Smith P. S., Sitko M. L. Optical polarimetry of PKS 2155-304 and constraints on accretion disk models for BL Lacertae objects // Astrophys. J.—1991.—383, N 2.—P. 580—586.

Smith P. S. et al. Optical and Hubble Space Telescope ultraviolet spectropolarimetry of 3C 273 and PG 1114+445 // Astrophys. J.—1993a.—409, N 2.—P. 604—611.

Smith P. S. et al. First ultraviolet spectropolarimetry of radio-selected BL Lacertae objects // Astrophys. J.—1993b.—415, N 2.—P. L83—L86.

Smith P. S. et al. Ultraviolet spectropolarimetry of Mrk 231 // BAAS.—1994.—26, N 2.—P. 967.

Somerville W. B. et al. Ultraviolet interstellar polarization observed with the Hubble Space Telescope // Astrophys. J.—1994.—427, N 1.—P. L47—L50.

Sparks W. B. et al. Hubble Space Telescope observations of synchrotronjets // Astrophys. J. Suppl.—1994.—90, N 2.—P. 909—916.

Spencer R. S. et al. Fabrication of optical components for the ultraviolet spectrometer and polarimeter on the Solar Maximum Mission // Opt. Eng.—1985.—24, N 3.—P. 548—554.

Stecher P. The wavelength dependence of interstellar polarization in the direction of ξ Ophiuchi // Bull. Amer. Astron. Soc.—1972.—4, N 2.—P. 270.

Steinmetz D. L. et al. A polarizer for the vacuum ultraviolet // Appl. Opt.—1967.—6, N 6.—P. 1001—1004.

Stenflo J. O. et al. Ultraviolet polarimeter to record resonance-line polarization in the solar spectrum around 130—150 nm // Appl. Opt.—1976.—15, N 5.—P. 1188—1198.

Stenflo J. O. et al. Search for spectral line polarization in the solar vacuum ultraviolet // Solar Phys.—1980.—66, N 1.—P. 13—19.

Steshenko N. V. On Polarimetric Observation in the SPECTRUM-UV Mission. SPECTRUM-UV Project Documents. March, 1996.

Taylor M. et al. First ultraviolet spectropolarimetry of hot supergiants // Astrophys. J.—1991.—382, N 2.—P. L85—L87.

Thomson R. C. et al. Internal structure and polarization of the optical jet of the quasar 3C 273 // Nature.—1993.—365, N 6442.—P. 133—135.

Webb W. et al. The wavelength dependence of polarization of active galaxies and quasars // Astrophys. J.—1993.—419, N 2.—P. 494—514.

Whittet D. C. B. et al. Ultraviolet interstellar polarization observed with the Hubble Space Telescope // First Symposium on the Infrared Cirrus and Diffuse Interstellar Clouds. — 1994.—P. 88—90.

Wolff M. J. et al. Ultraviolet interstellar linear polarization. I. Applicability of current dust gruin model. Astrophys. J.—1993.—403, N 2.—P. 722—735.

Wolinski K. G. The ultraviolet polarization of X-ray binary systems observed with the Hubble Space Telescope // PASP.—1994.—106, N 703.—P. 1019.

Wolinski K. G. et al. The polarization of X-ray binaries in the ultraviolet. I. Cygnus XR-1, 4U 0900-40, and 4U 1700-37 // Astrophys. J.—1996.—457.—P. 859—867.

Woodgate B. E. et al. The ultraviolet spectrometer and polarimeter on the Solar Maximum Mission // Solar Phys.—1980.—65, N 1.—P. 73—90.

CONTENTS